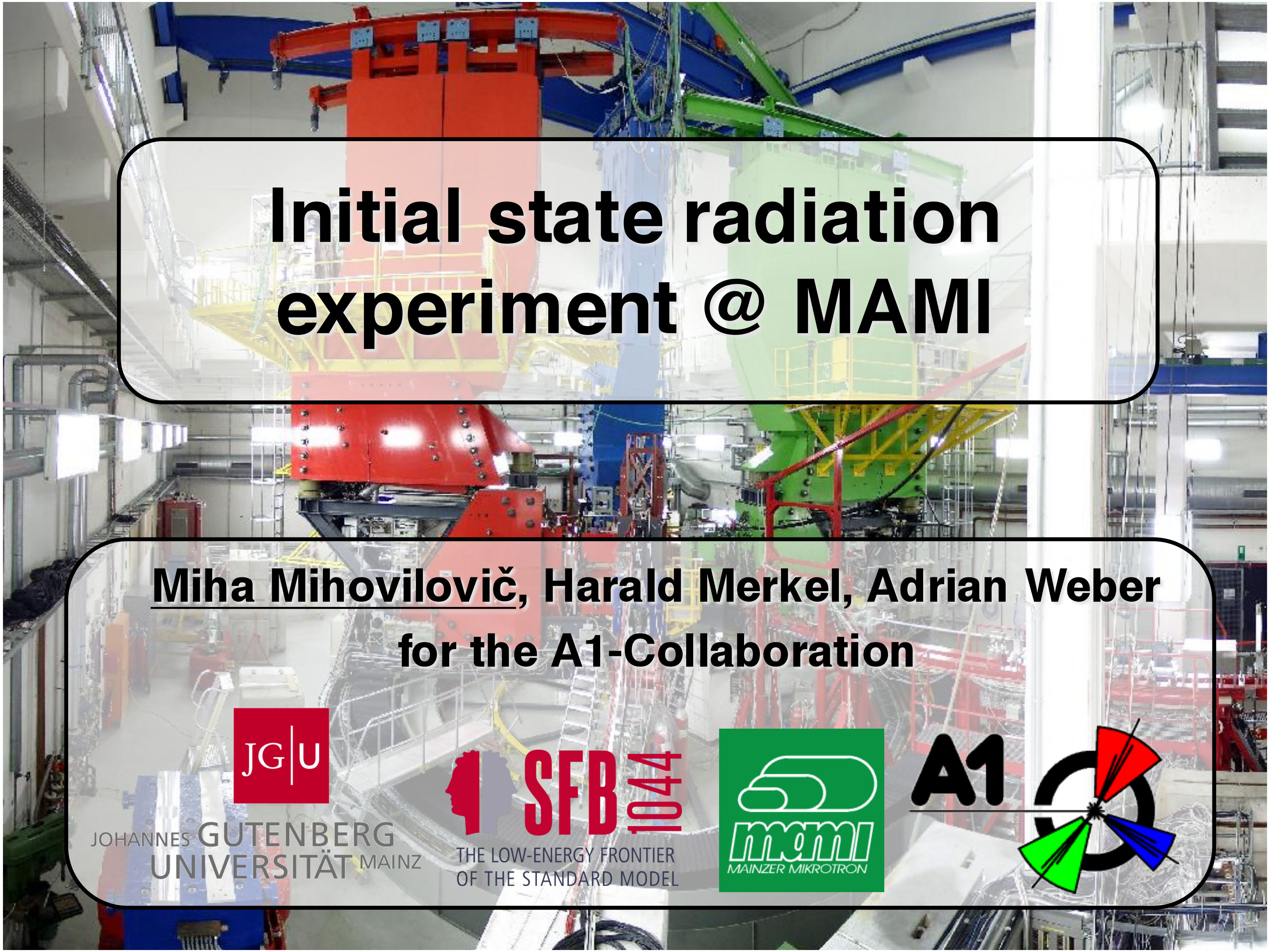

Initial state radiation experiment @ MAMI

Miha Mihovilovič, Harald Merkel, Adrian Weber

for the A1-Collaboration

JOHANNES GUTENBERG UNIVERSITÄT MAINZ

SFB 1044 THE LOW-ENERGY FRONTIER OF THE STANDARD MODEL

mami MAINZER MIKROTRON

A1

What is the size of the proton?

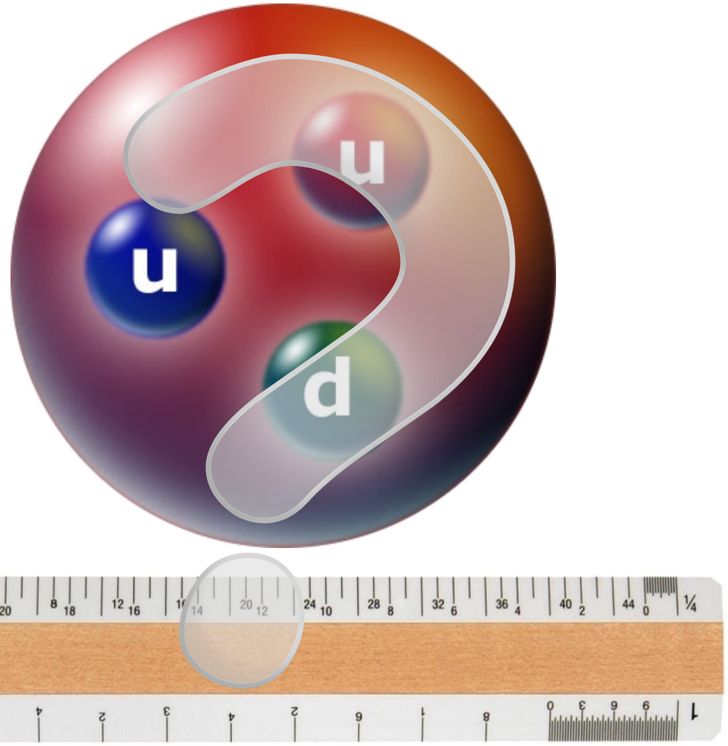

1963

2014

After 50 year of research is the size of the proton still
not understood to a desirable accuracy!

The proton radius puzzle

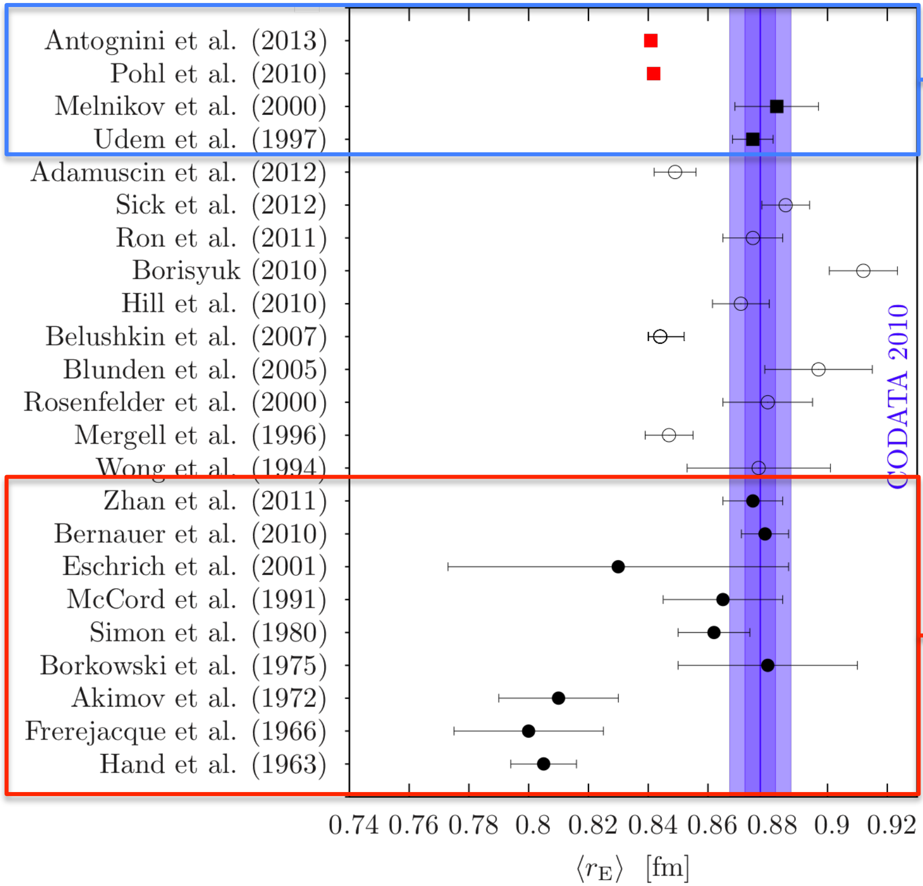

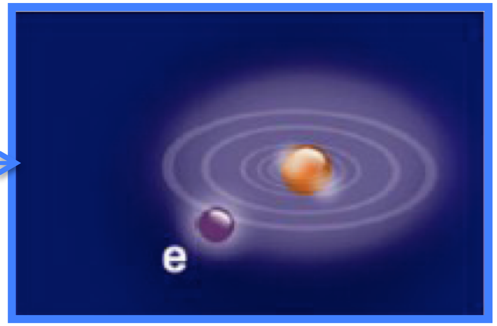

Atomic spectroscopy

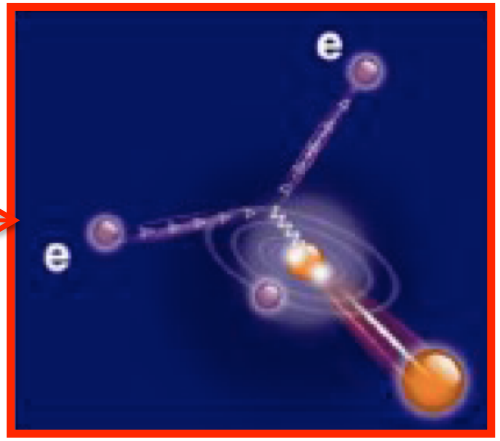

V. Sulkosky

Scattering experiments

- Many different measurements done through the years.

- New μ-p Lamb shift measurement, 7σ away.

- Further investigations necessary.

Elastic Cross-Section measurement

- Radius can be obtained by measuring cross section of H(e,e')p:

$$\frac{d\sigma}{d\Omega} = \left(\frac{d\sigma}{d\Omega}\right)_{Mott} \frac{1}{1+\tau}\left[G_E^2(Q^2) + \frac{\tau}{\varepsilon} G_M^2(Q^2)\right]$$

$$\varepsilon = \left[1 + 2(1+\tau)\tan^2\frac{\vartheta_e}{2}\right]^{-1} \qquad \tau = \frac{Q^2}{4m_p^2},$$

- Extraction of FF via Rosenbluth, Super-Rosenbluth Separation:

$$G_E(Q^2) \approx G^{Dipole}(Q^2) = \left(1 + \frac{Q^2}{0.71}\right)^{-2}$$

- Best estimate for radius:

$$\left\langle r_E^2 \right\rangle = -6\hbar^2 \frac{d}{dQ^2} G_E(Q^2)\Big|_{Q^2=0}$$

$$\rho_{Dipole}(r) = \frac{1}{8\pi}\left(\frac{12}{\langle r_E^2\rangle}\right)^{\frac{3}{2}} \exp\left(-r\sqrt{\frac{12}{\langle r_E^2\rangle}}\right)$$

No data at lowest Q^2. Determination of proton radius depends on the slope of FF (Q^2->0).

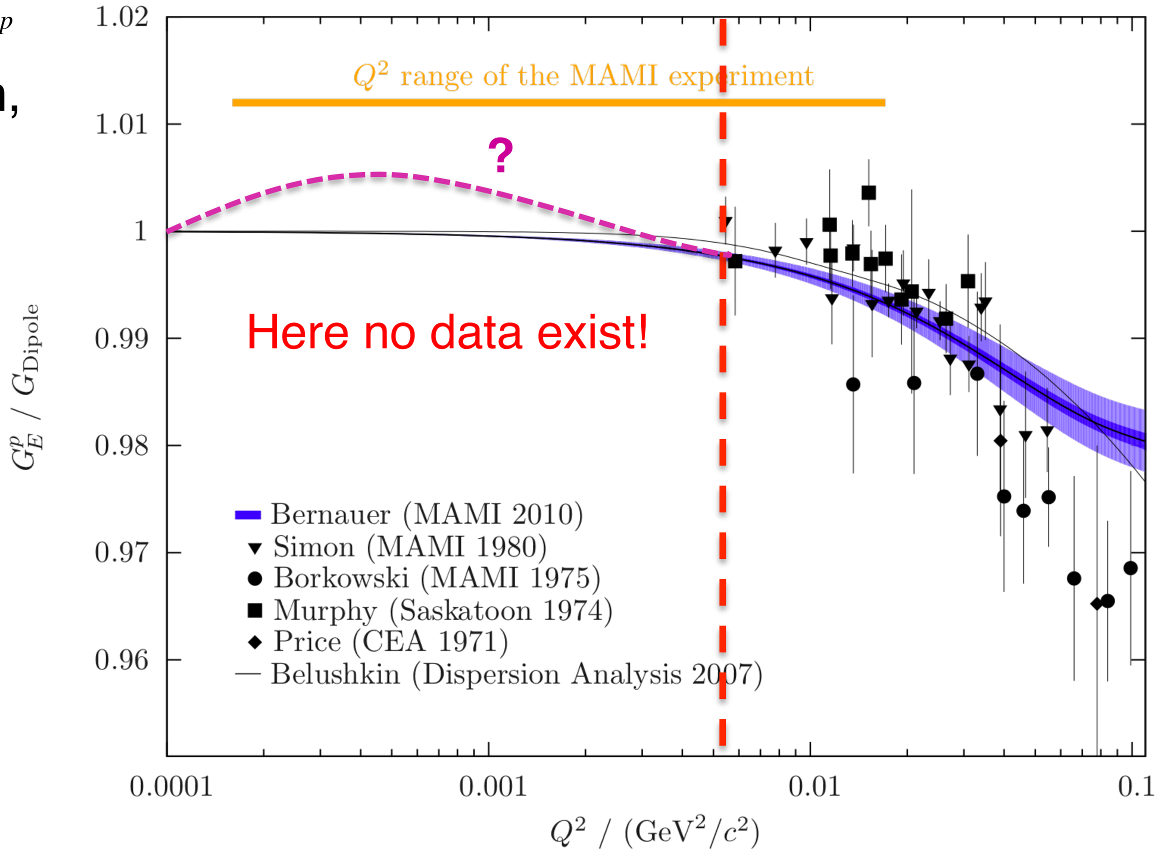

Exploiting the radiative tail

- To test the behavior of FFs at $Q^2 \sim 0$, elastic cross-section measurements at lower Q^2 would be needed.

- Lowest Q^2 is constrained by the limitations of experimental apparatus (beam energy, scattering angle …).

WAY AROUND: Use information stored in the radiative tail.

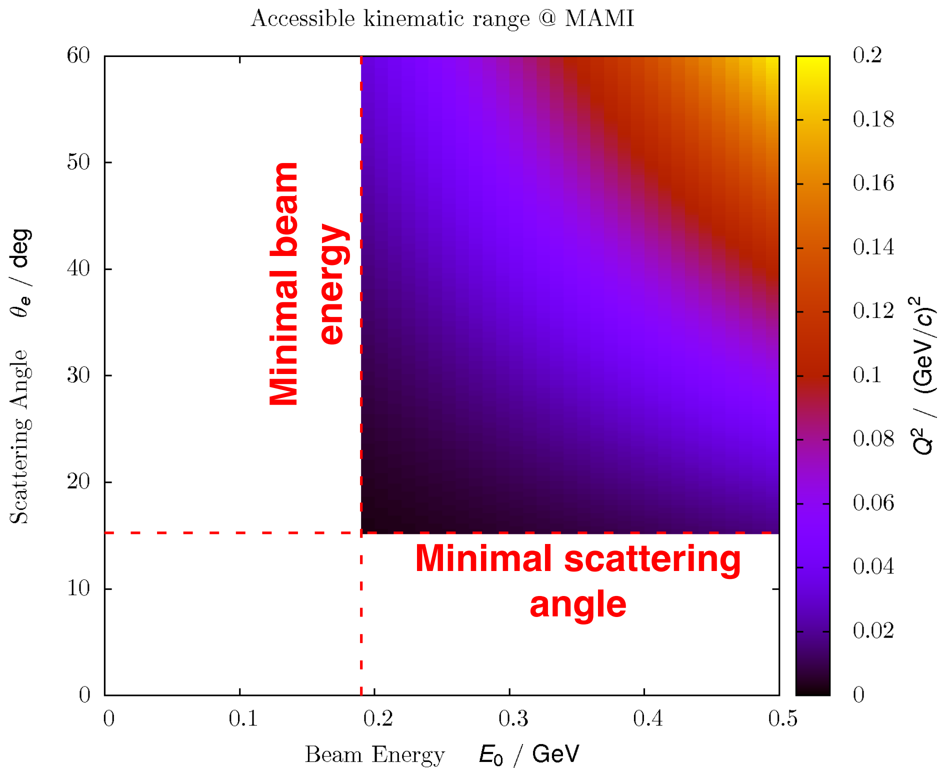

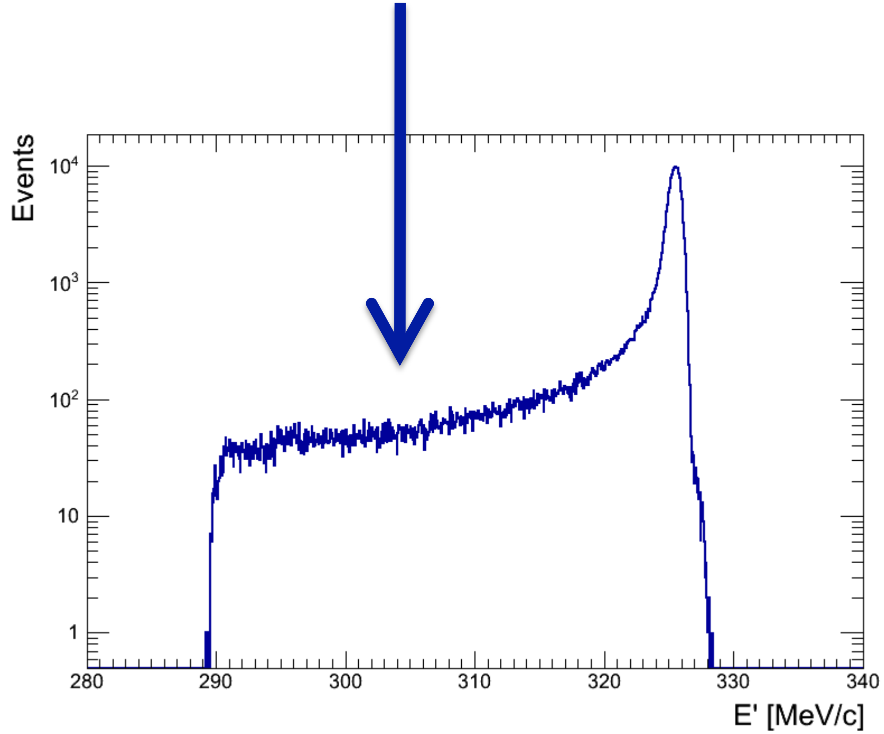

Initial state radiation

- Radiative tail dominated by coherent sum of two Bethe-Heitler diagrams.

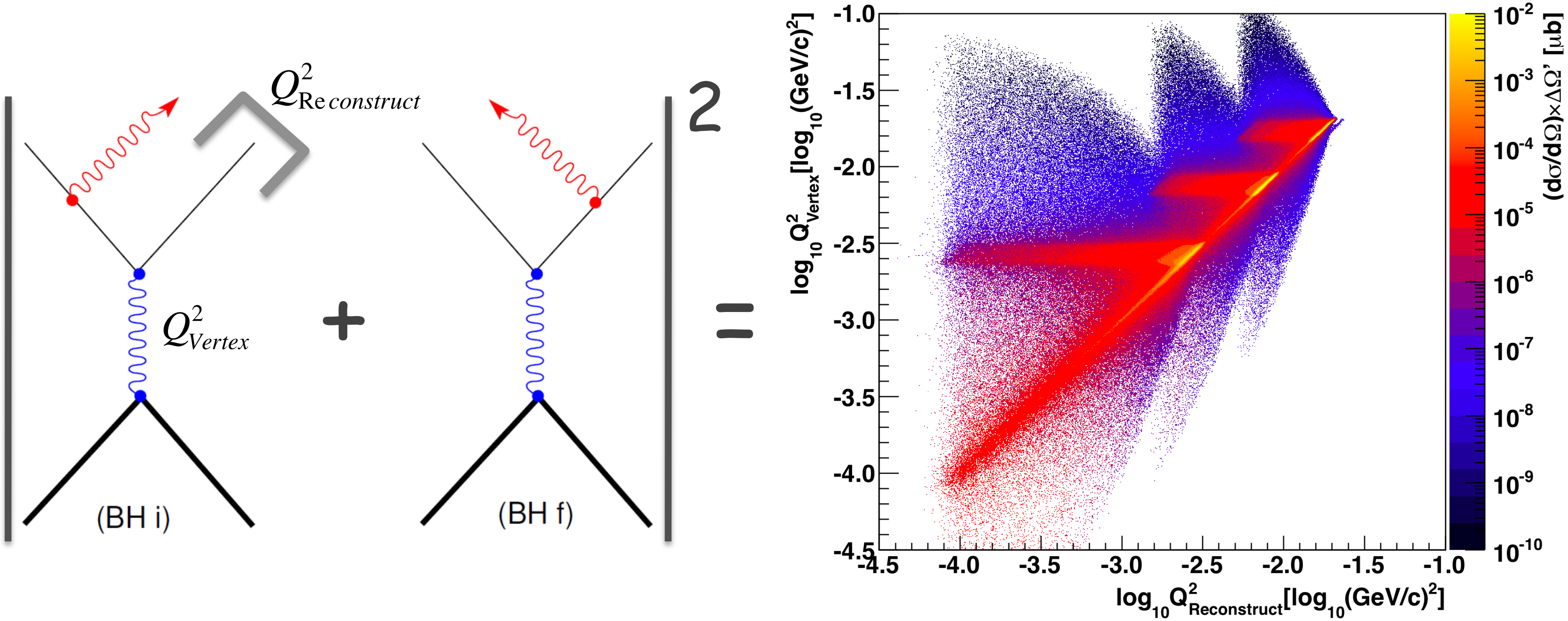

- In data ISR can not be distinguished from FSR.
- **Combining data to the simulation, ISR information can be reached**.
- Idea behind new MAMI experiment to extract $\mathbf{G_e^p}$ at $\mathbf{Q^2 \sim 10^{-4}\ (GeV/c)^2}$
- Redundancy measurements at higher Q^2 for testing this approach in a region, where FFs are well known.

Simul++

- In the experiment **the G_e^p will not be directly extracted** from data.

- <u>FF are camouflaged</u> by effects that accompany FSR and ISR diagrams (Born diagrams, vertex corrections).

- Approach analogous to Bernauer et al. will be used, where **simulated distributions are directly compared to measured data**.

- Simulate **ep->epγ** with a sophisticated Monte-Carlo simulation `Simul++`.

- Simulation will be run with various values of G_E^p. Contribution of G_M^p is neglected @ Q^2~0.

- Final values of FFs will be determined by a χ^2-minimization.

Searching for G_e^p which gives the best agreement between data and simulation

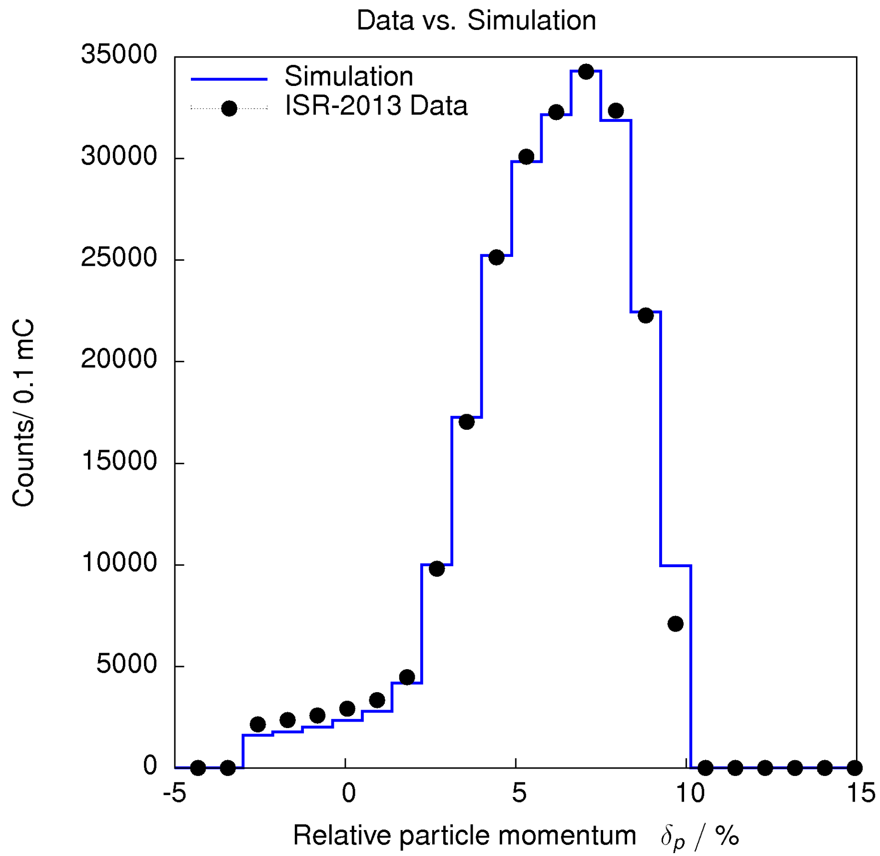

Going beyond simple approximation

- Simul++ employs an advanced event generator, **which exactly calculates amplitudes for four leading order diagrams.**

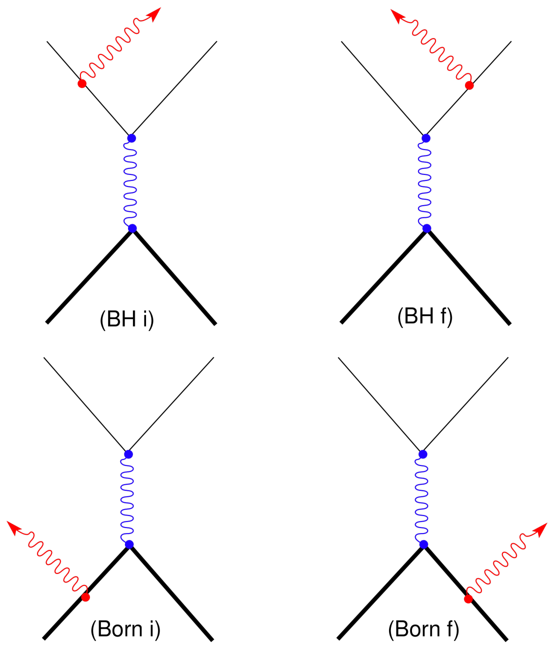

- Precise spectrometer acceptances, particle energy-losses and rescatterings are also implemented.

- Next order terms considered via effective correction to the cross-section.

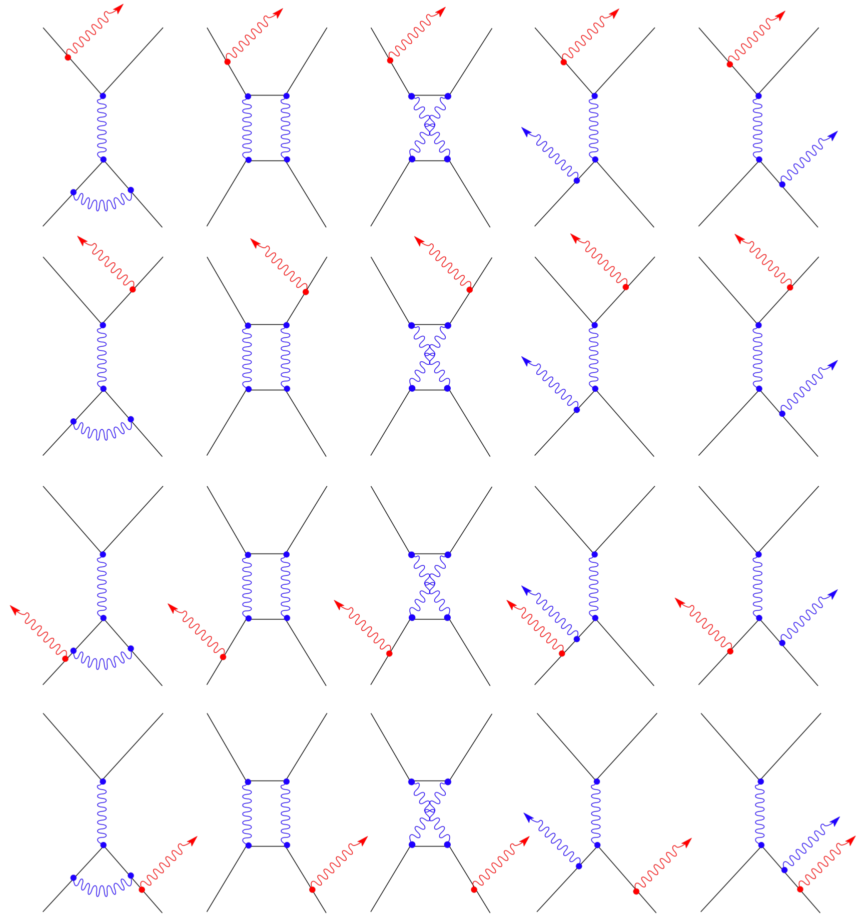

First experiment

- First measurements done in 2010. Three weeks of data taking. (2 weeks with full target, 1 week with empty target)
- **Purpose:** Is the experiment feasible? Discover potential problems.

Electron Beam:

- Energy: 195, 330, 495 MeV
- Current: 10nA – 1µA
- Rastered beam

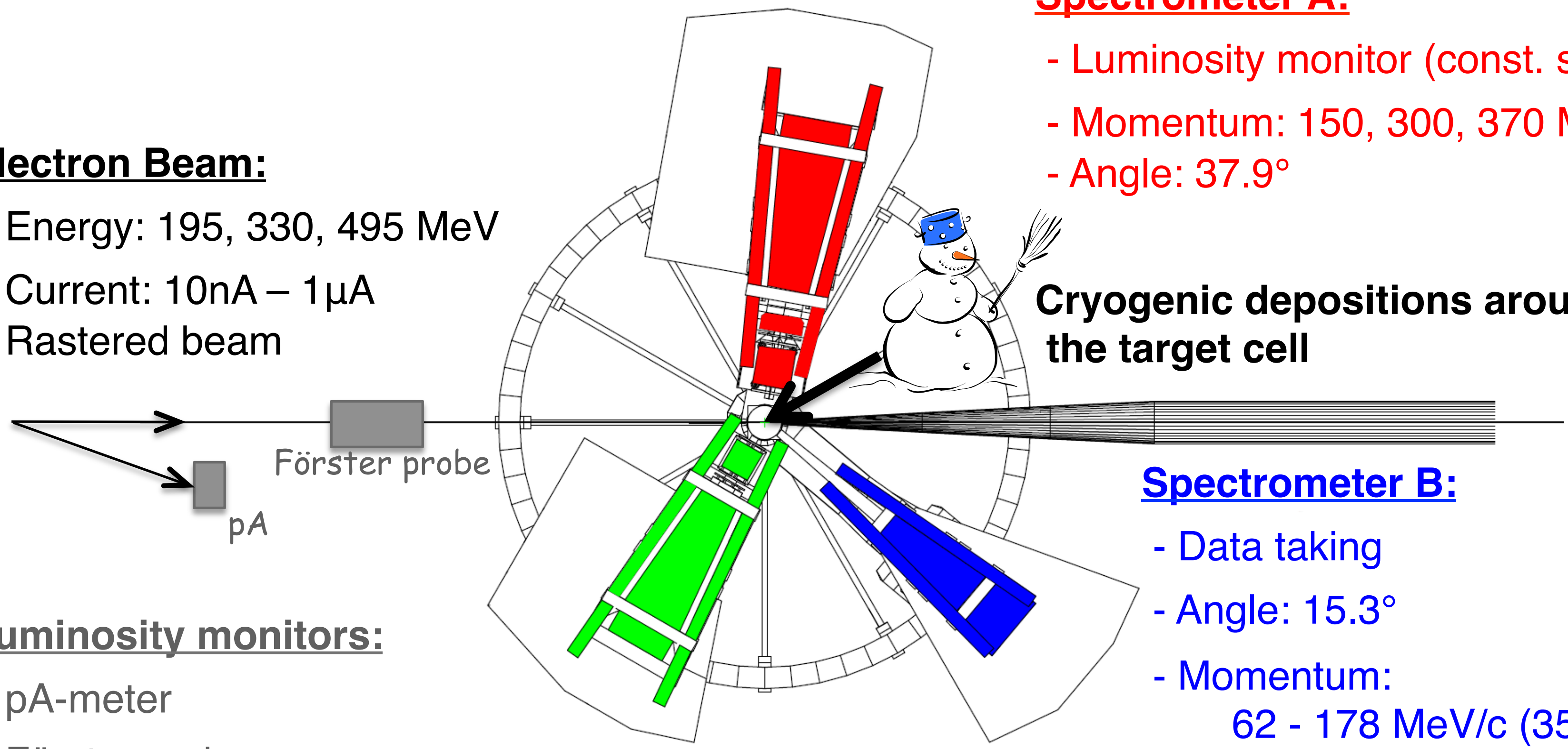

Spectrometer A:

- Luminosity monitor (const. setting)
- Momentum: 150, 300, 370 MeV/c
- Angle: 37.9°

Cryogenic depositions around the target cell

Spectrometer B:

- Data taking
- Angle: 15.3°
- Momentum:
  62 - 178 MeV/c (35 setups)
  167 - 313 MeV/c (9 setups)
  236 - 468 MeV/c (16 setups)

Luminosity monitors:

- pA-meter
- Förster probe

Spectrometer C:

- Not used

Major handicap of the pilot experiment

- Experiment utilizes a standard Liquid-Hydrogen target.

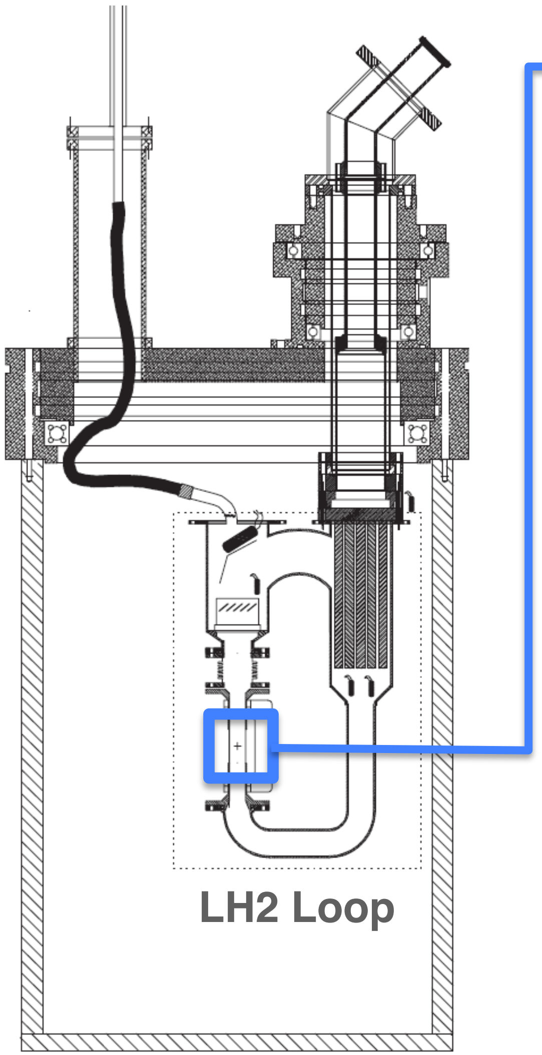

Scattering chamber

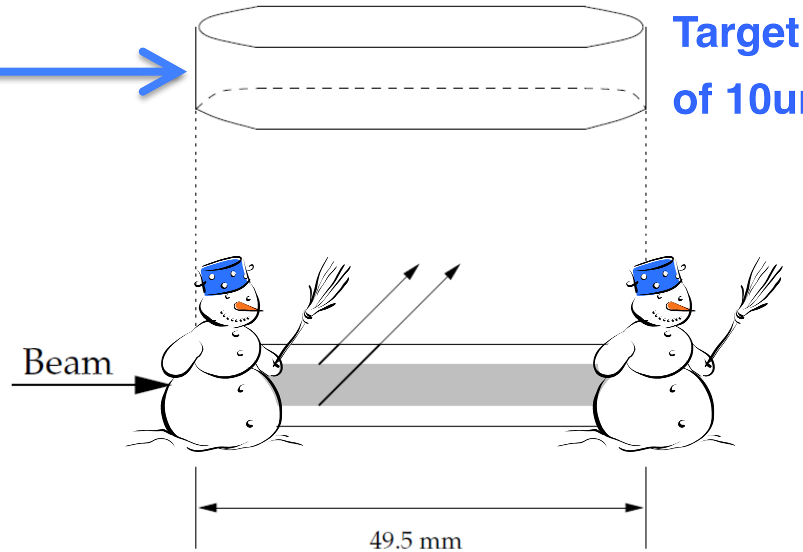

Target Cell made of 10um Havar

- Due to <u>poor vacuum and low beam intensities</u>, layer of **Cryogens covered the target cell**.
- Depositions consists of residual N_2, O_2 and H_2O.
- Affects not only particle energy-losses but changes also the detection rates.
- Disturbs Luminosity determination.
- Amount of snow <u>changes irregularly with time.</u>

Effects of cryogenic depositions

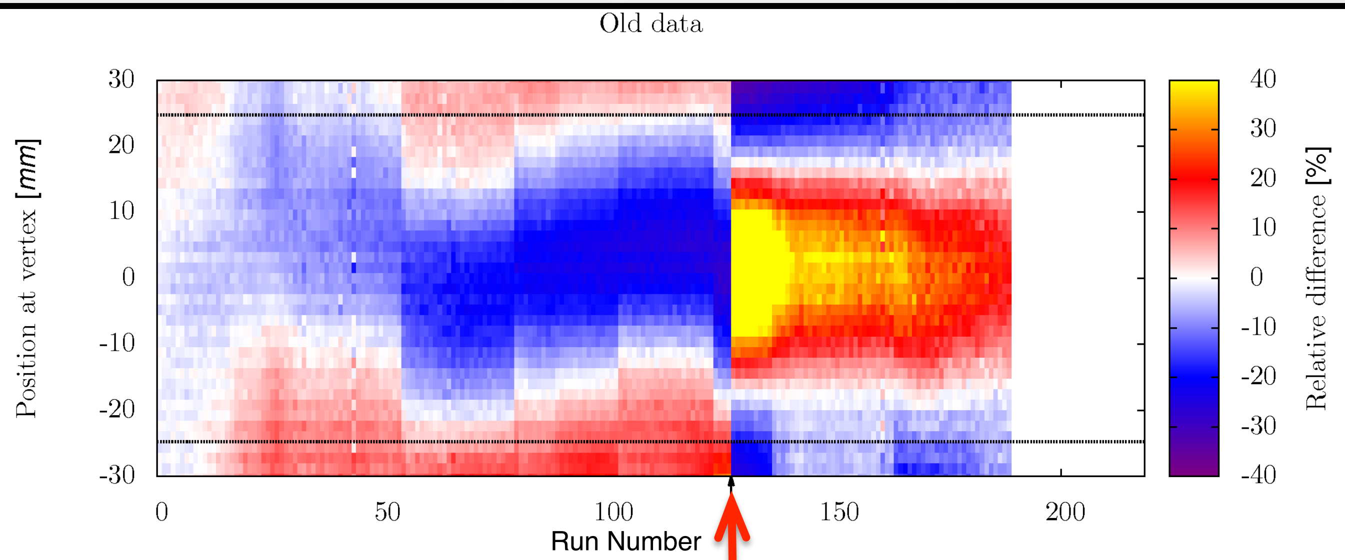

High current run that melts cryogenic depositions

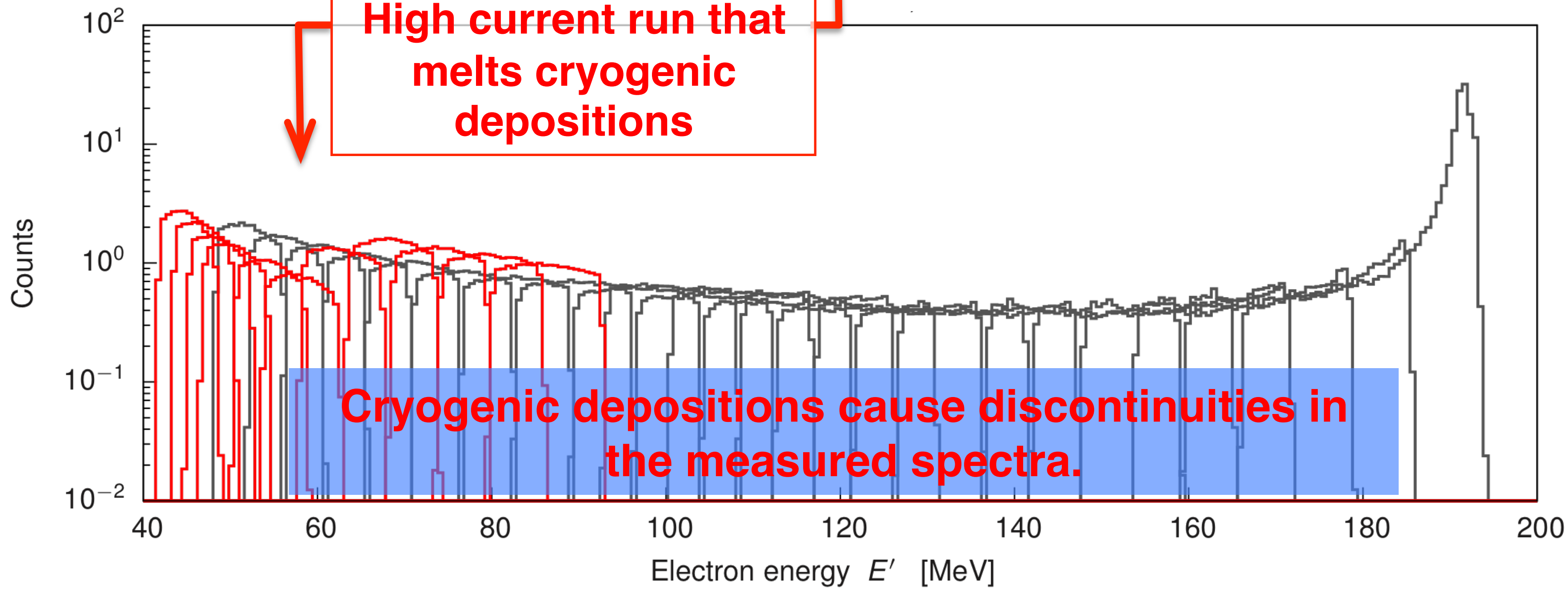

Full experiment

- Full experiment done in August 2013. Four weeks of data taking.

Electron Beam:

- Energy: 195, 330, 495 MeV
- Current: 10nA – 1µA
- Rastered beam

Spectrometer A:

- Luminosity monitor (const. setting)
- Momentum: 180, 305, 386 MeV/c
- Angles: 50°, 60°

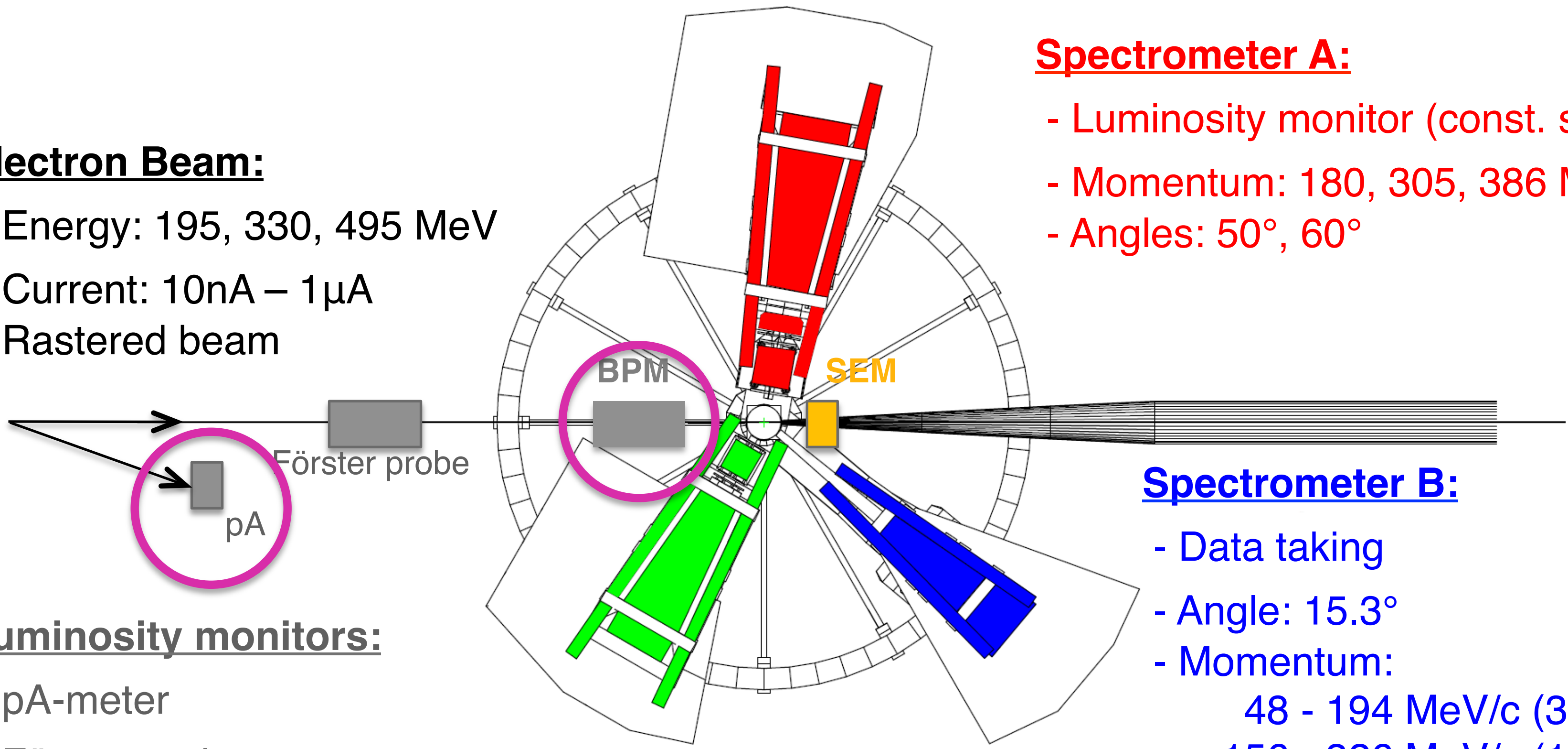

Spectrometer B:

- Data taking
- Angle: 15.3°
- Momentum:
  - 48 - 194 MeV/c (35 setups)
  - 156 - 326 MeV/c (12 setups)
  - 289 - 486 MeV/c (9 setups)

Luminosity monitors:

- pA-meter
- Förster probe
- SEM

Spectrometer C:

- Not used

Beam control module:

- Communicates with MAMI and ensures very stable beam.
- BPM and pA-meter measurements performed automatically every 3min.

Minimizing cryogenic depositions

- **<u>Improved vacuum</u>** in target chamber ($10^{-4} \rightarrow 10^{-6}$ mbar).

- New target windows with additional layer of Aramid.

- Fixing Spectrometer A to elastic settings to see effects of snow gathering more clearly.

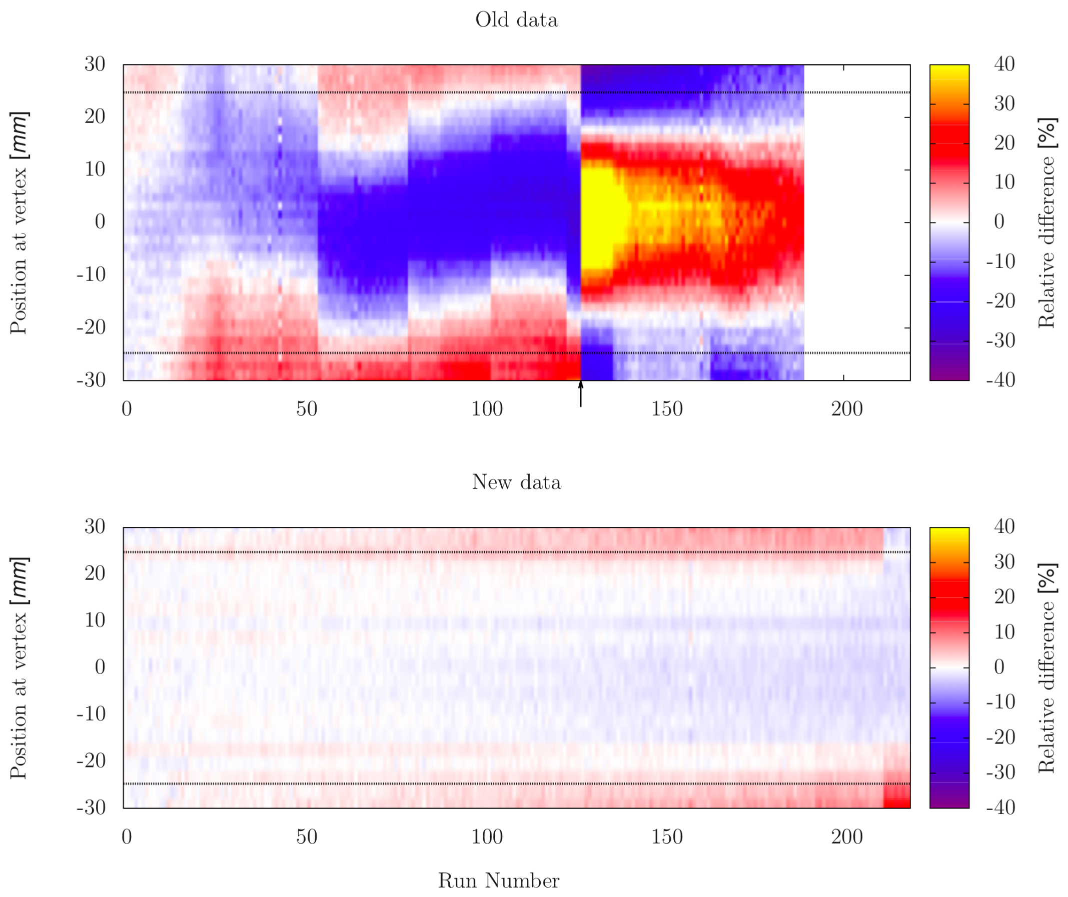

Spectrometer A has enough resolving power for clear identification of Nitrogen and Oxygen.

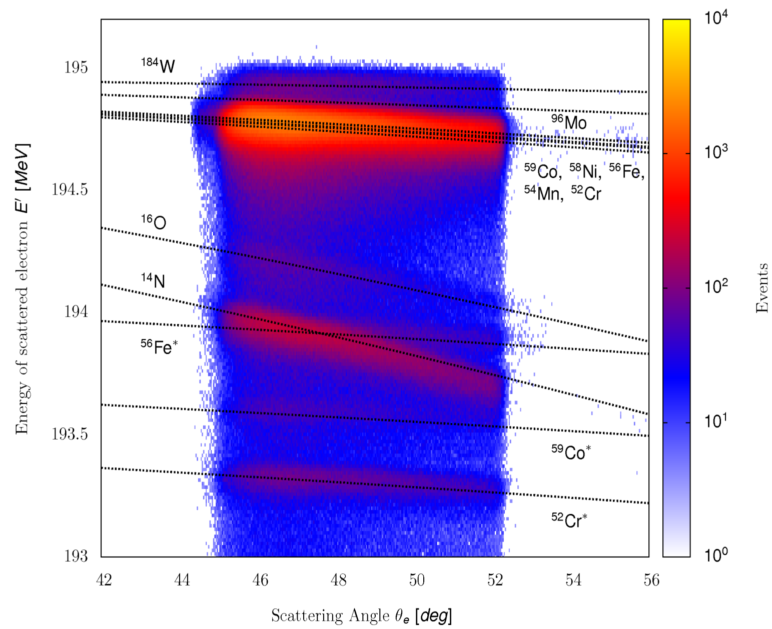

First Results

- First findings of online analysis.
- Data are normalized to 0.1mC using Förster probe & Spec-A.
- Only acceptance and Vertex-z cuts considered.
- Pion production processes contribute ~10% at smallest momenta.
- Visible effects of finite resolution. (wall contributions still present)
- **Agreement between data and simulation justifies use of `Simul++`.**

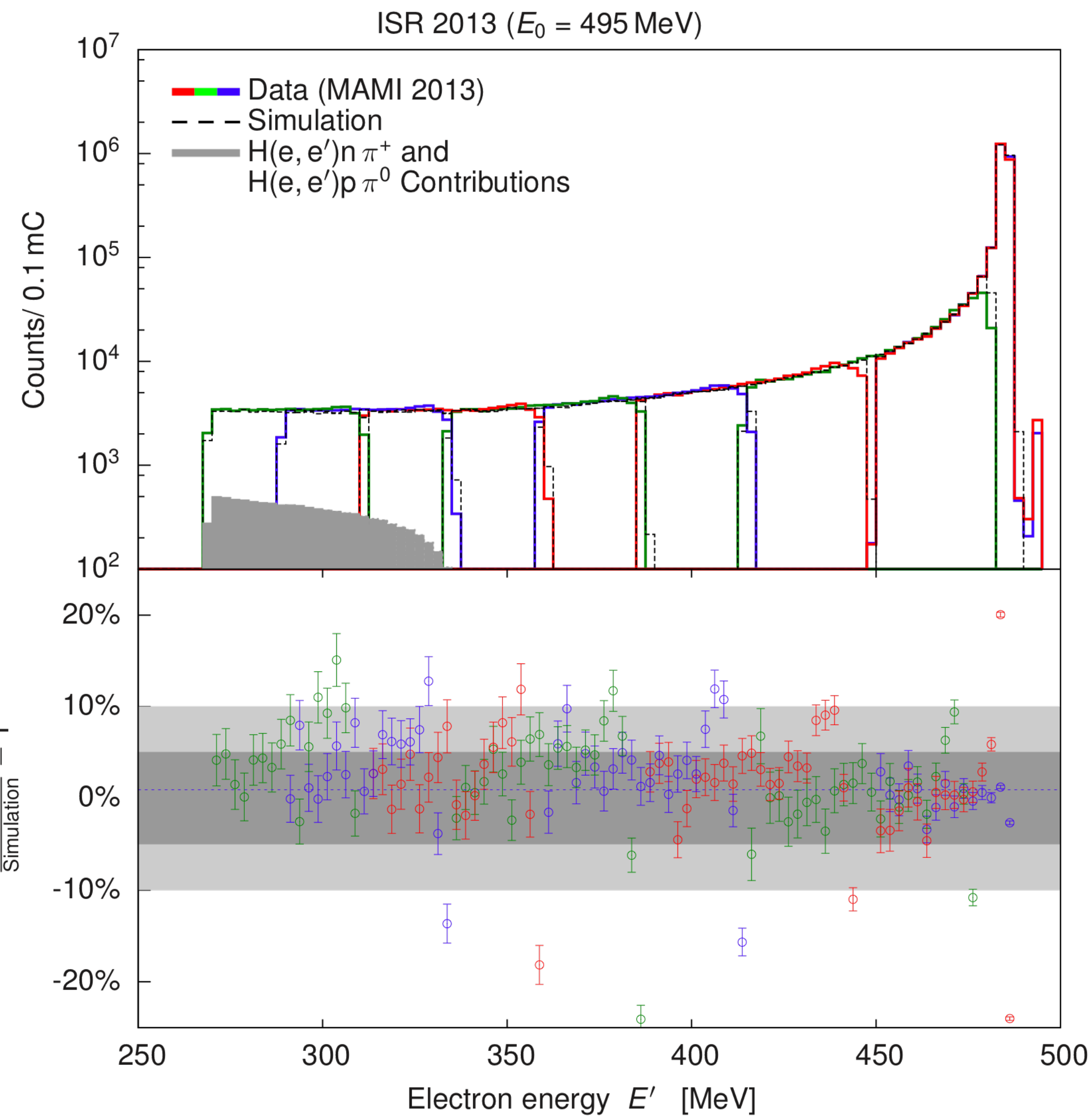

First Results #2

- First findings of online analysis.
- Data are normalized to 0.1mC using Förster probe & Spec-A.
- Only acceptance and Vertex-z cuts considered.
- Pion production processes contribute ~10% at smallest momenta.
- Visible effects of finite resolution. (wall contributions still present)
- **Agreement between data and simulation justifies use of `Simul++`.**

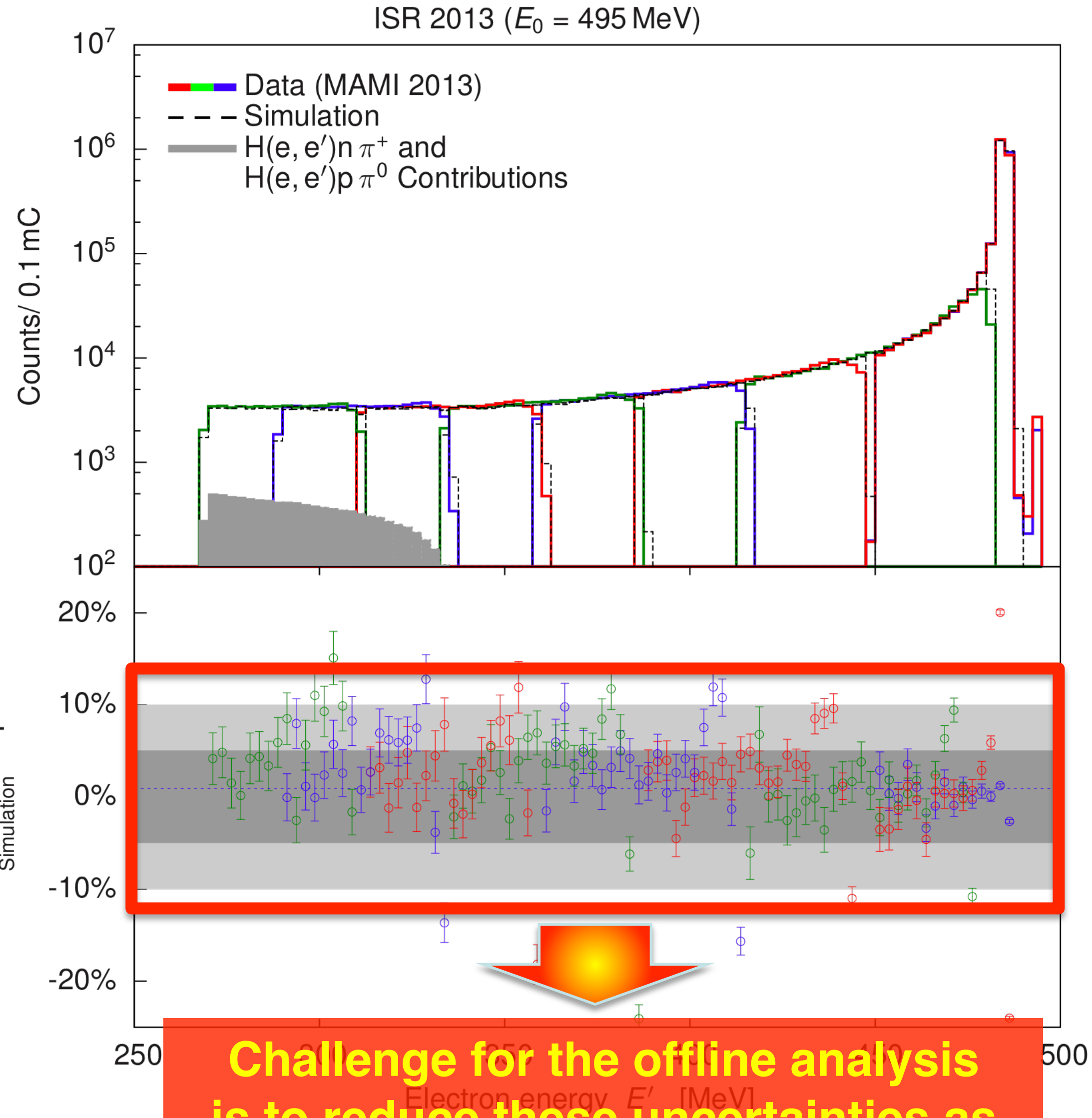

Challenge for the offline analysis is to reduce these uncertainties as much as possible!

Challenges for the offline analysis

- **Goal:** determine the cross-sections with **accuracy of ~ 1%.**
- All steps of the analysis must be prudently performed.

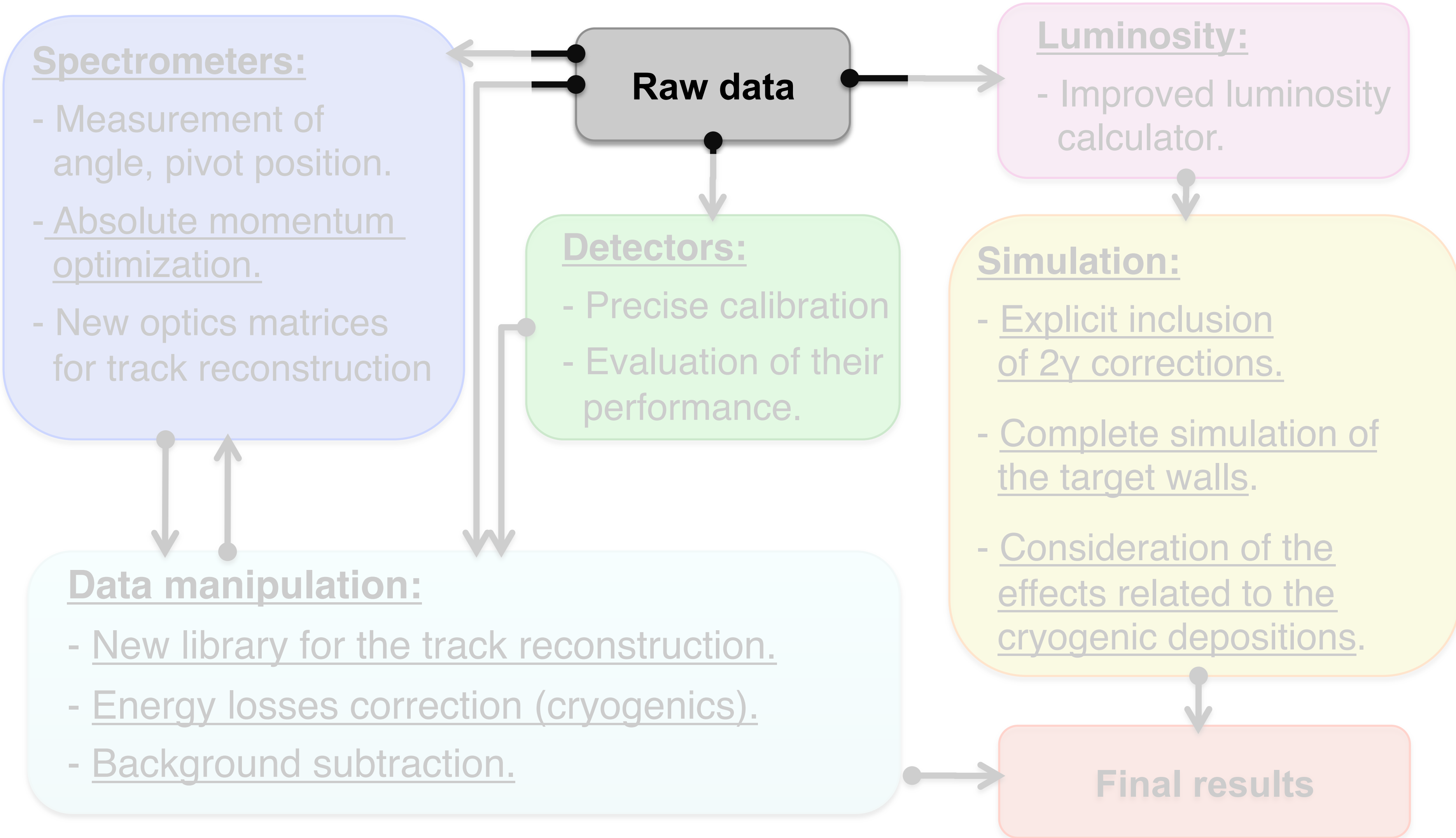

Challenges for the offline analysis

- **Goal:** determine the cross-sections with **accuracy of ~ 1%.**
- All steps of the analysis must be prudently performed.

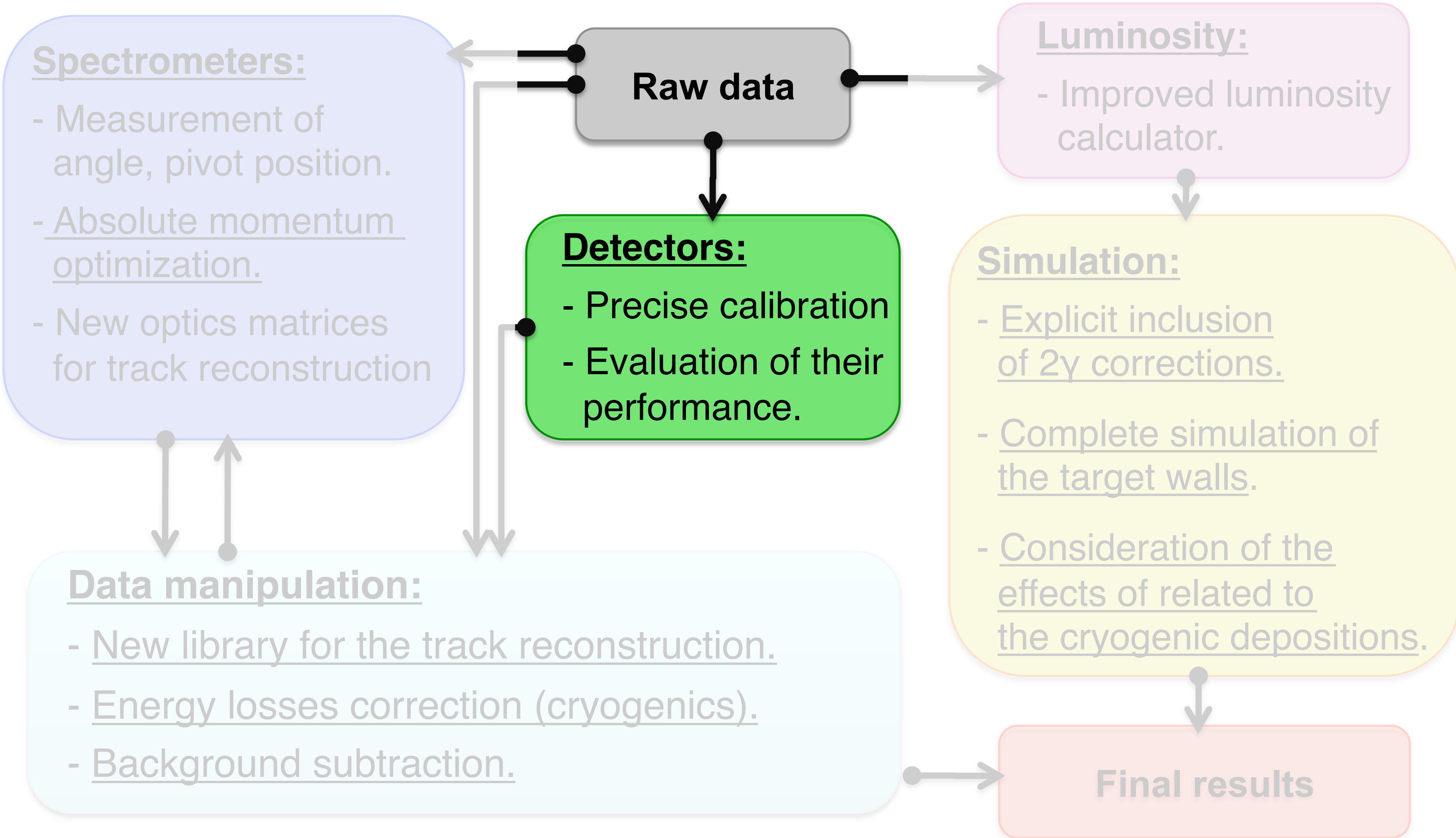

Detector calibration and evaluation

- **Cherenkov detector:** Pedestal subtraction and alignment of the ADC. Determination of the detection efficiency (99%).

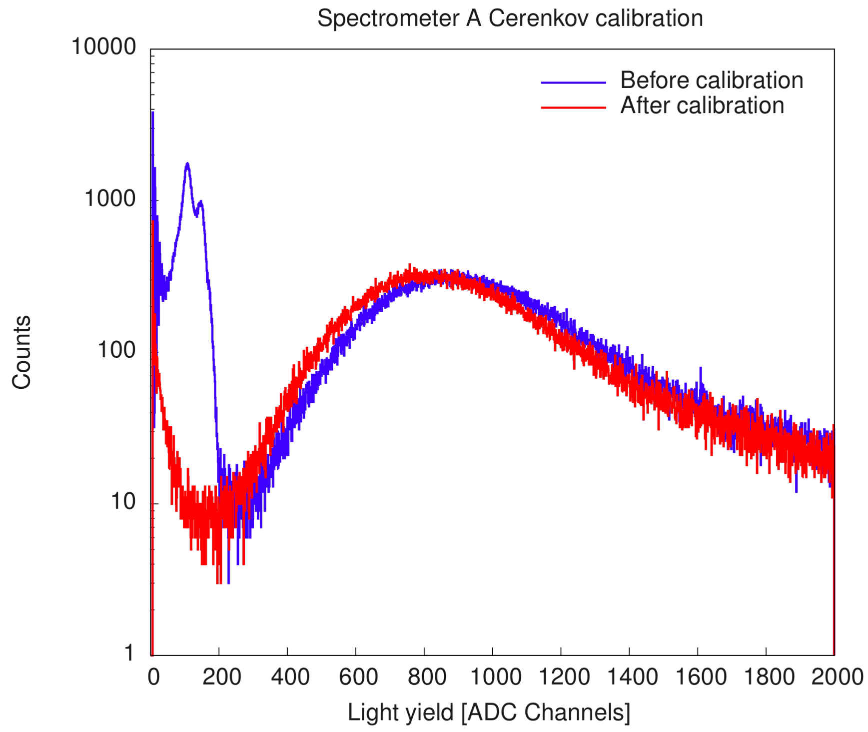

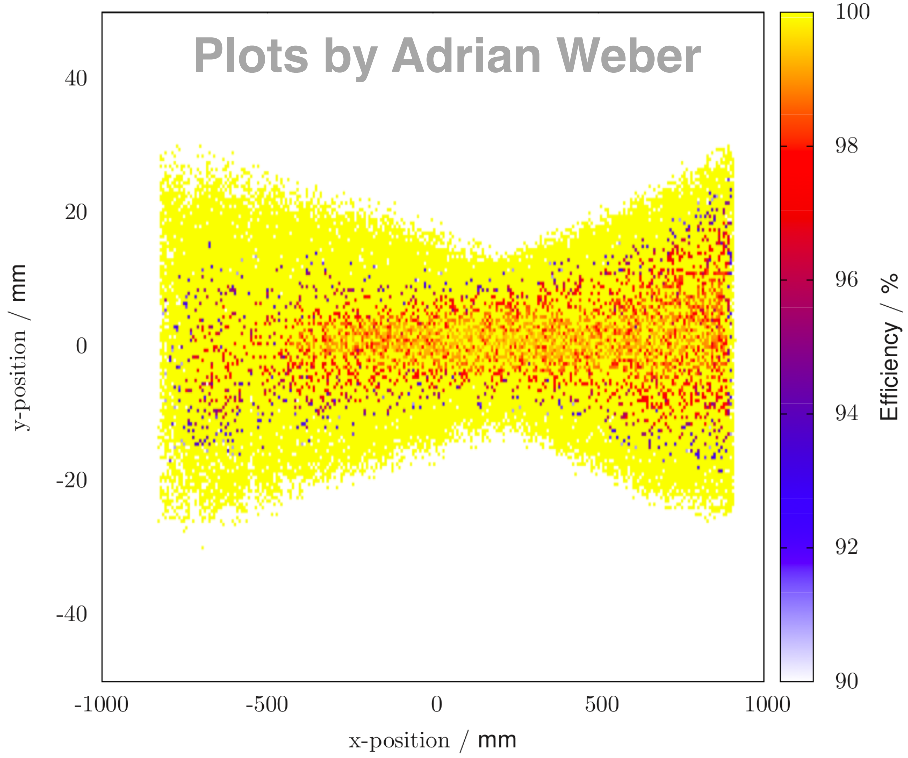

- **Scintillation detectors:** Detection efficiency determination (≥ 98 %).

- **VDC:** Precise efficiency studies revealed a room for improvements. New analysis library for the improved track reconstruction efficiency.

Challenges for the offline analysis

- **Goal:** determine the cross-sections with **accuracy of ~ 1%.**
- All steps of the analysis must be prudently performed.

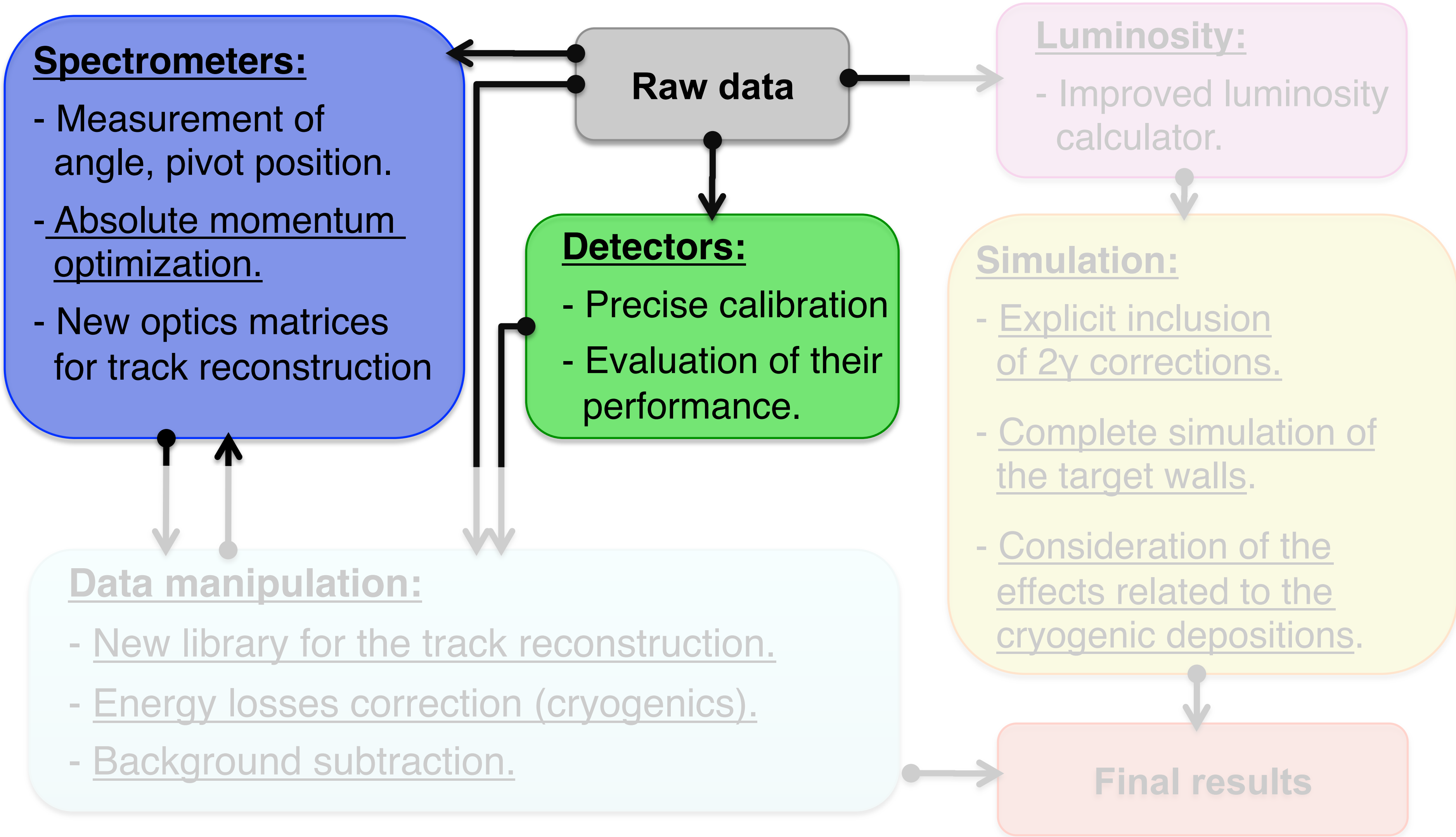

Improved Spectrometer optics

- Dedicated 3-week optics calibration beam time.
- Data collected for all three considered beam energies.
- Broadening due to multiple scattering effects in the air and foils.

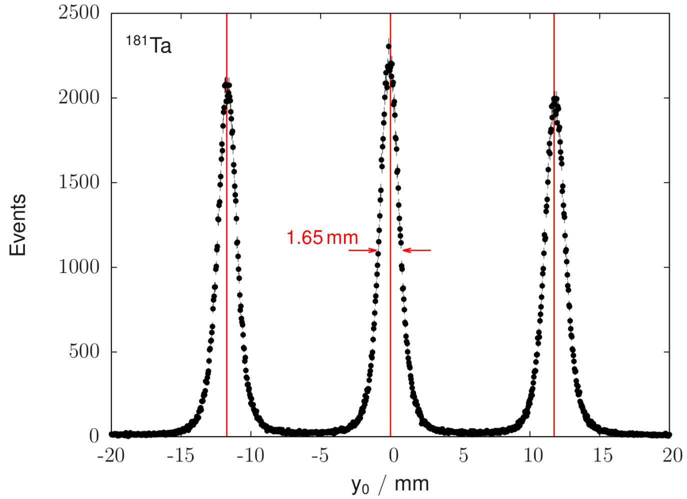

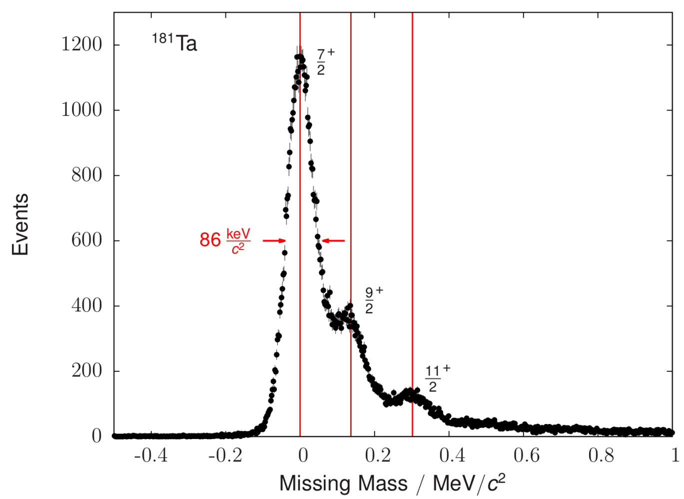

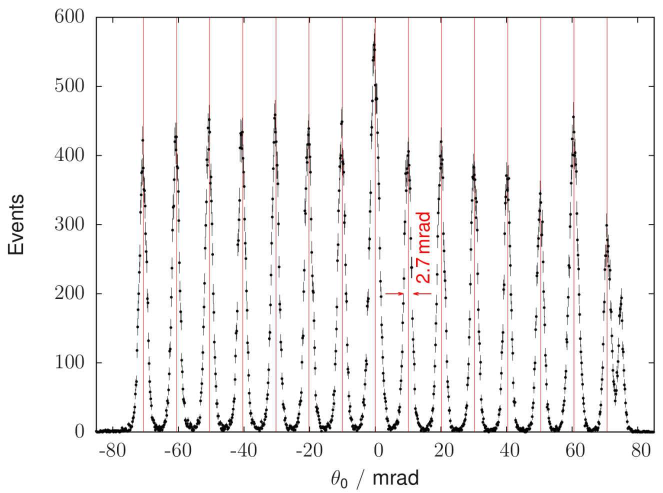

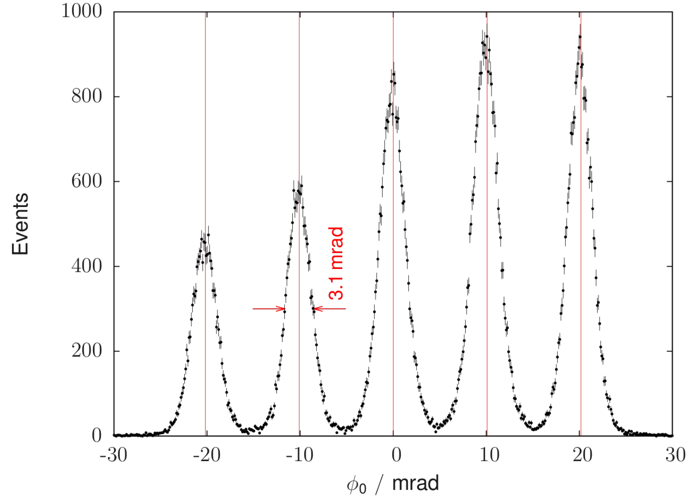

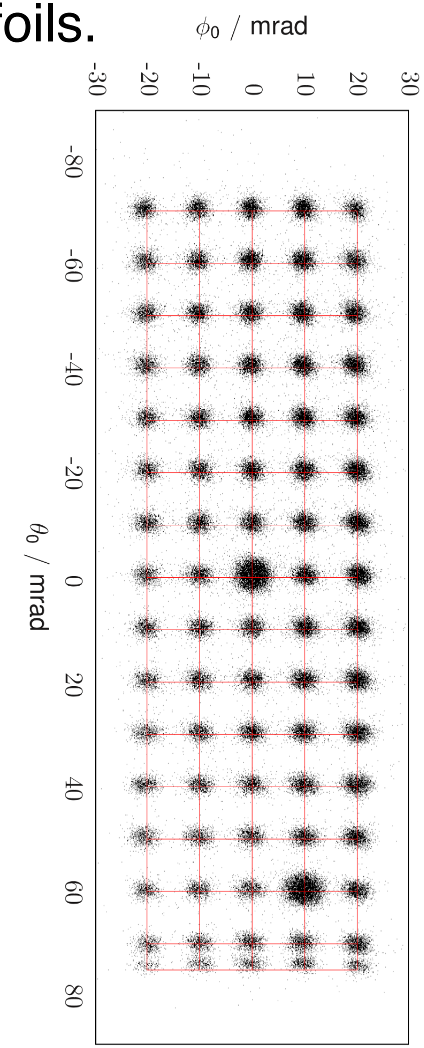

Challenges for the offline analysis

- **Goal:** determine the cross-sections with **accuracy of ~ 1%.**
- All steps of the analysis must be prudently performed.

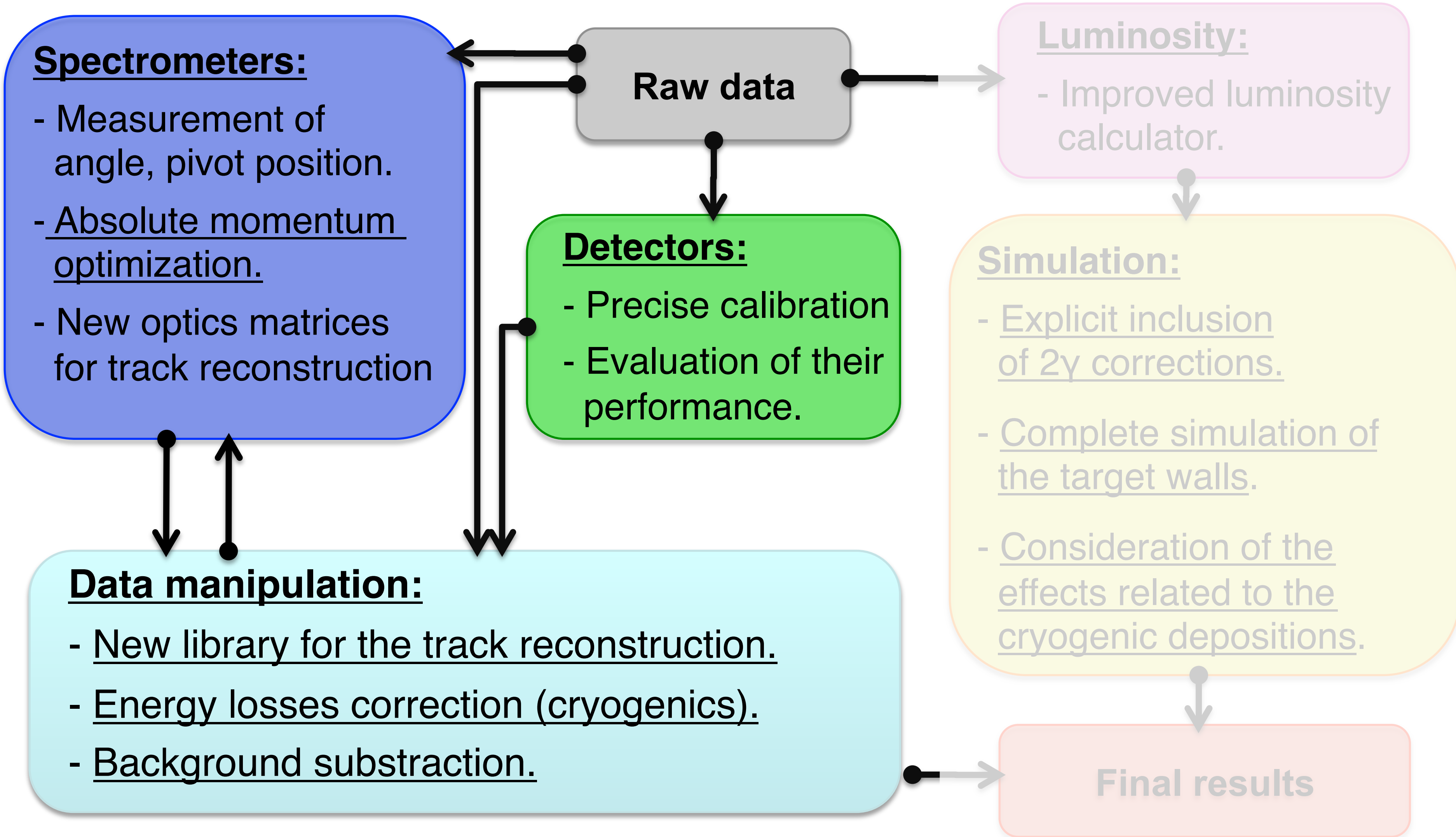

Background subtraction

- Subtraction of the empty cell data:

With the decreasing momentum the vertex resolution deteriorates.

Vertex cuts can no longer be successfully applied.

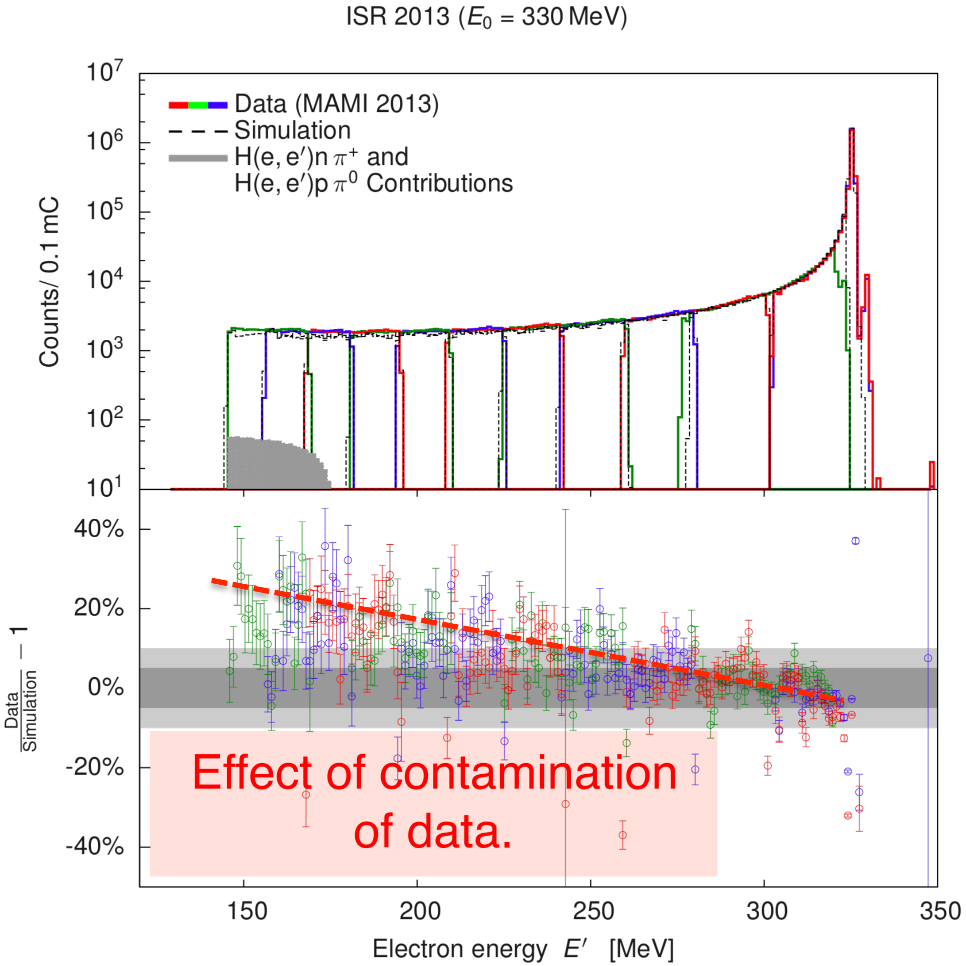

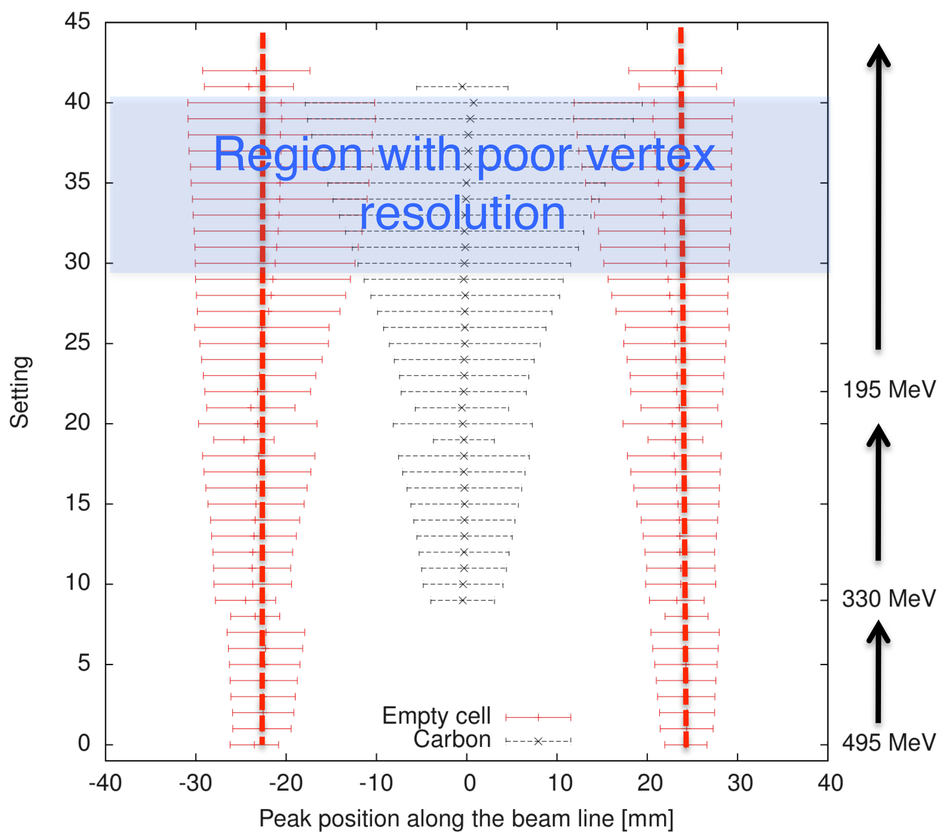

Subtraction of the cell walls

- At low momenta vertex resolution insufficient for successful vertex cuts.
- LH2 data contaminated with events from walls.
- Empty cell data required. They need to be tuned to full data!

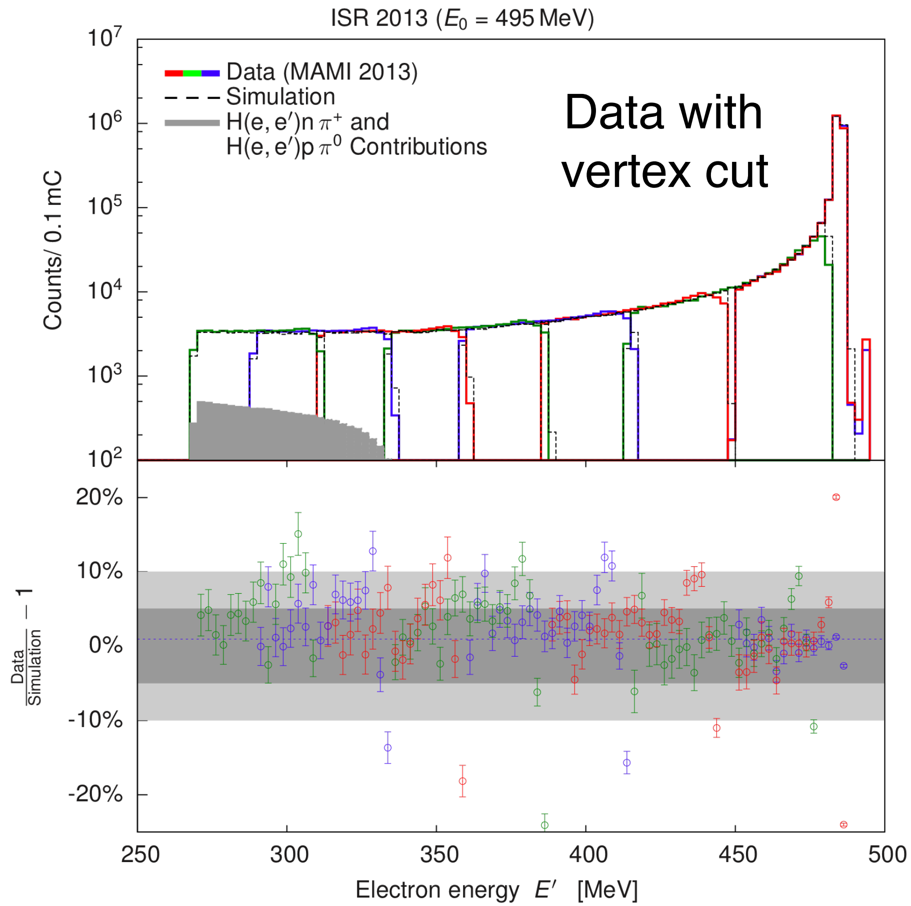

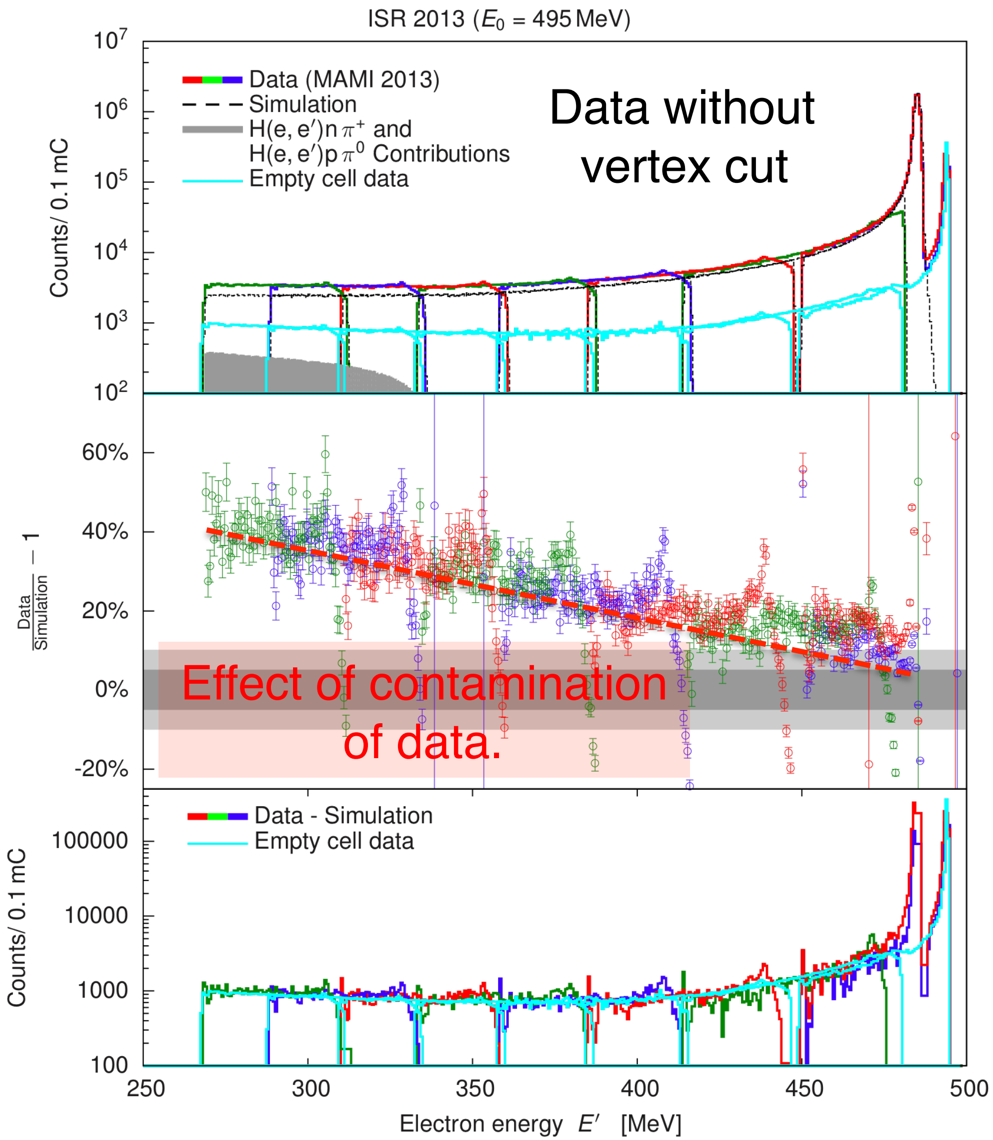

Challenges for the offline analysis

- **Goal:** determine the cross-sections with **accuracy of ~ 1%.**
- All steps of the analysis must be prudently performed.

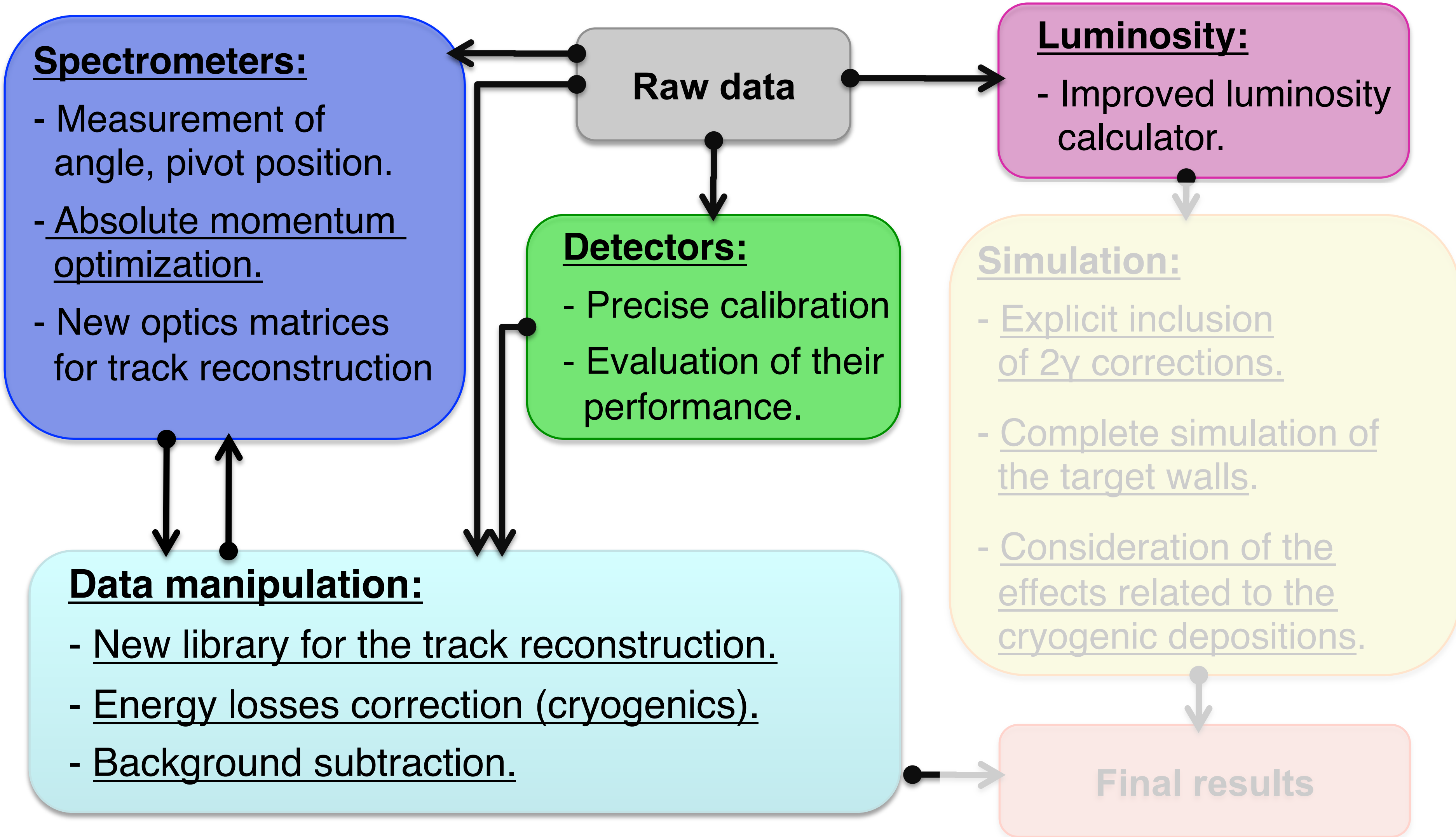

Challenges for the offline analysis

- **Goal:** determine the cross-sections with **accuracy of ~ 1%.**
- All steps of the analysis must be prudently performed.

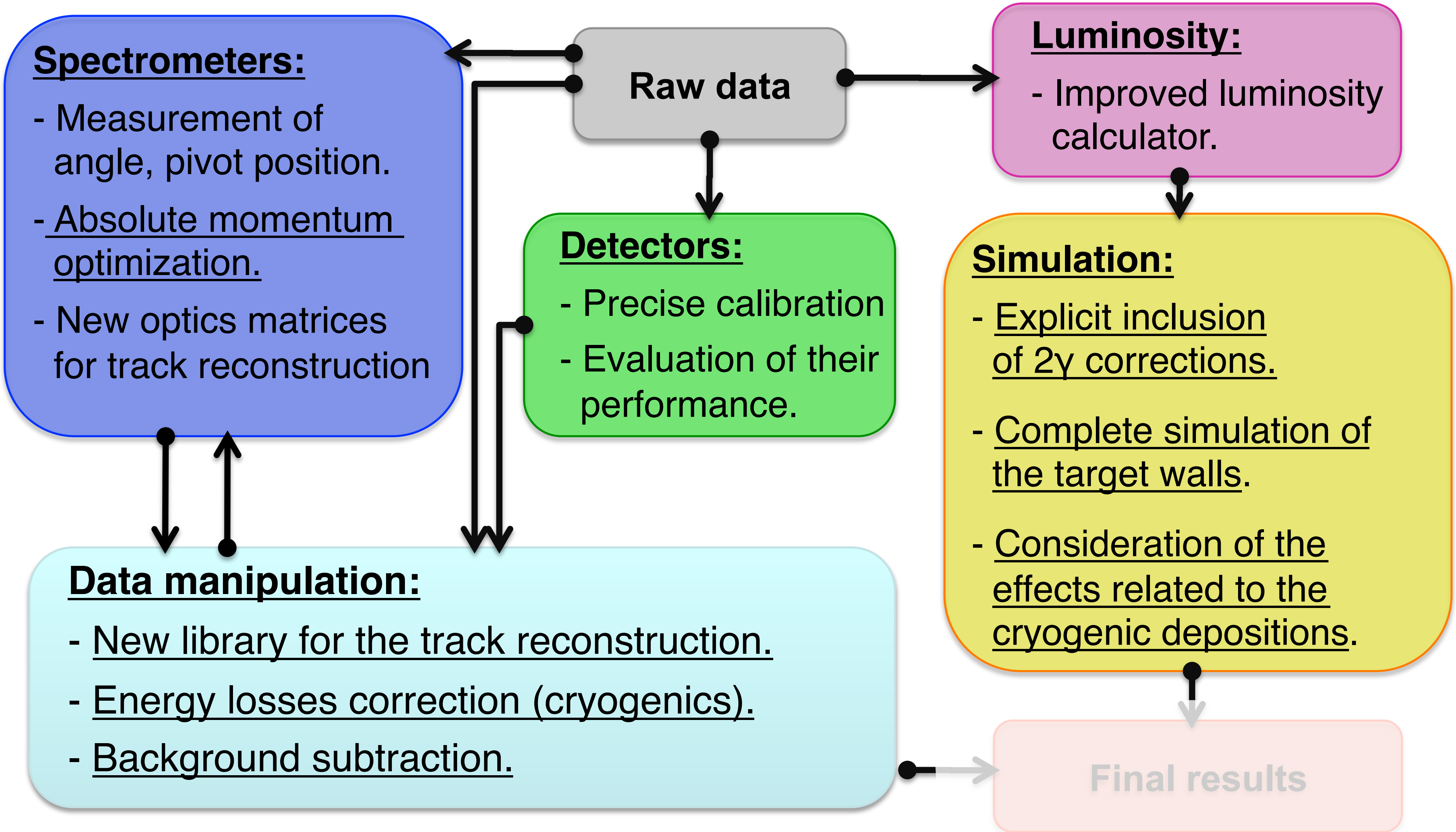

Challenges for the offline analysis

- **Goal:** determine the cross-sections with **accuracy of ~ 1%.**
- All steps of the analysis must be prudently performed.

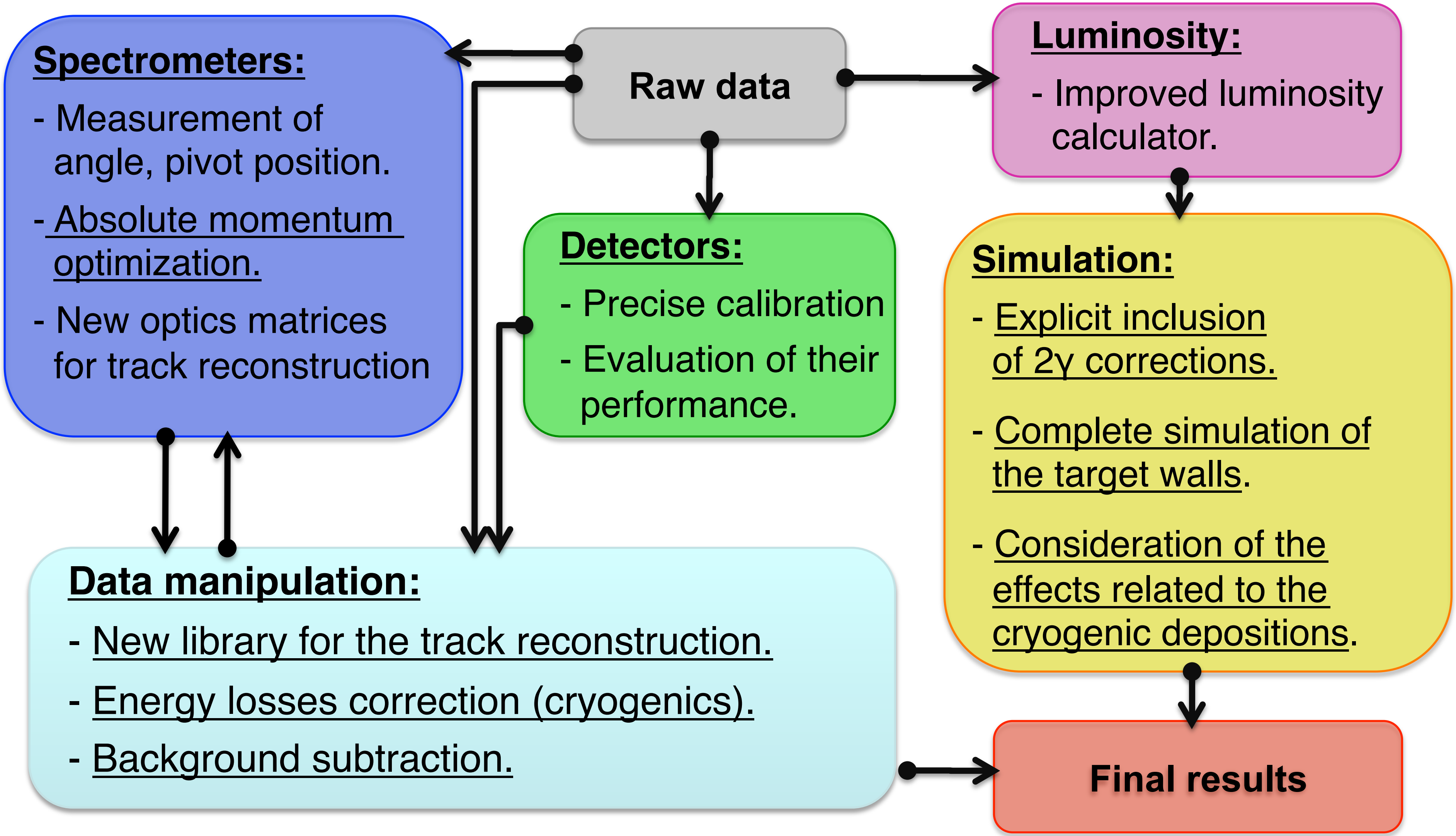

Conclusions

- Proton radius puzzle is an important open question of nuclear physics.

- First test measurements in 2010 proved the principle and revealed some experimental problem.

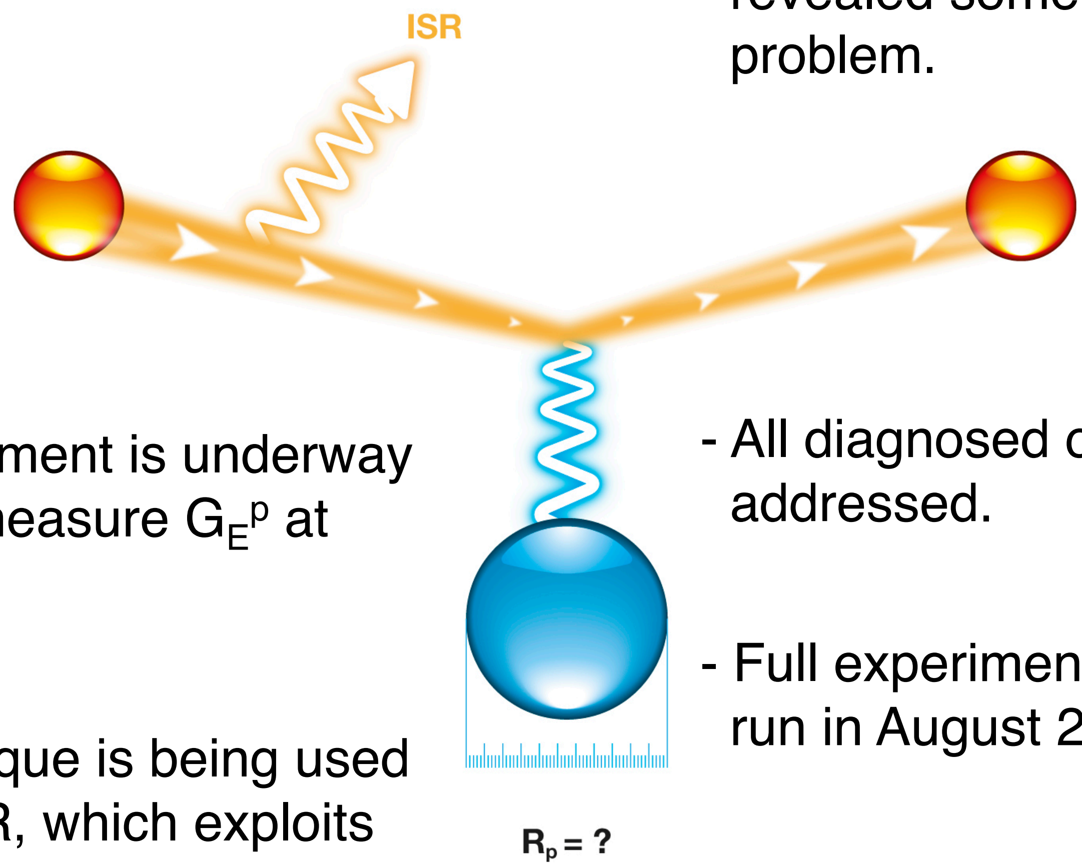

- A new experiment is underway at MAMI to measure G_E^p at very low Q^2.

- A new technique is being used based on ISR, which exploits information from radiative tail to determine FF at lowest Q^2.

- All diagnosed obstacles were addressed.

- Full experiment was successfully run in August 2013.

- **Data analysis is now underway.**


Thank you !

Solid state ^{12}C data

- Old data showed discontinuities in the measured missing mass spectra.
- Effect most probably **consequence of cryogenic depositions**.
- Other explanations also possible (acceptance change at low missing momenta, other sources of background).
- Data with thin ^{12}C target used to inspect the performance and stability of the apparatus.

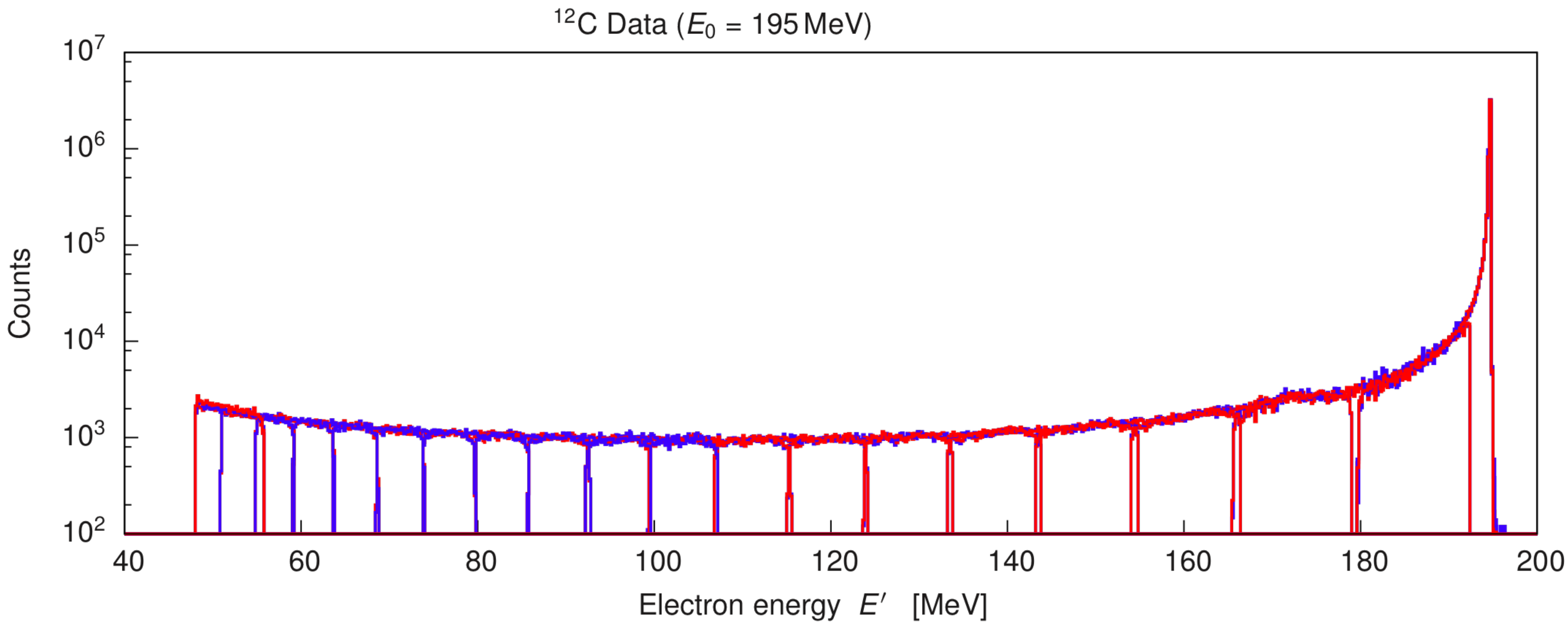

Kinematic settings of the full experiment

- Measured kinematic points and corresponding Q^2 at vertex.
- Three kinematic regions overlap to verify ISR approach.